Mapping HIV mortality in six Latin American countries using incomplete vital registration systems

Michael Cork

A thesis

submitted in partial fulfilment of the

requirements for the degree of

Master of Public Health

University of Washington

2020

Committee:

Laura Dwyer-Lindgren

Simon I. Hay

University of Washington

Abstract

Mapping HIV mortality in six Latin American countries using incomplete vital registration systems

Michael Cork

Chair of the Supervisory Committee:

Laura Dwyer-Lindgren

Department of Health Metric Sciences

Background

HIV remains a public health priority in Latin America, but across the region HIV mortality is not in universal decline. While it is known that the burden of HIV is concentrated in urban areas and high-risk groups, detailed subnational estimates that cover multiple countries and years are lacking, due, in part, to incomplete vital registration systems and statistical challenges related to estimating mortality rates in areas with low numbers of HIV deaths.

Methods

Using vital registration (VR) data ranging from 2000 to 2017, we estimated the HIV mortality rate and the number of HIV deaths by age group, sex, and municipality in Brazil, Colombia, Costa Rica, Ecuador, Guatemala, and Mexico. We modelled HIV mortality using a Bayesian spatially explicit mixed-effects regression model that incorporates prior information on VR completeness. We calibrated our results to the Global Burden of Disease Study 2017.

Results

All countries displayed over a 40-fold difference in age-standardized HIV mortality between municipalities with the highest and lowest HIV mortality rate in the last year of study for men, and over a 20-fold difference for women. Despite decreases in HIV mortality in all countries—apart from Ecuador—across the period of study, we find broad variation in relative changes in HIV mortality at the municipality level and increasing relative inequality over time in all countries. National age patterns reflected shifts in mortality to older age groups over time and in the latest year of study, the median age group among those who died from HIV ranged by 5 to 15 years among countries at the municipality level. In all six countries included in this analysis, HIV deaths were concentrated in fewer than 10% of municipalities in the latest year of study.

Conclusions

Our subnational estimates of HIV mortality revealed significant spatial variation and diverging local trends in HIV mortality over time and by age group. This analysis provides a framework for incorporating data from incomplete VR systems and could be used to understand local needs and guide more geographically precise public health intervention to reduce HIV-related deaths.

Background

Human immunodeficiency virus (HIV) continues to be a large contributor to morbidity and mortality across the globe [1, 2]. While the HIV epidemic is largely concentrated in sub-Saharan Africa, HIV remains a public health priority in Latin America and the Caribbean where over 40,000 people were estimated to have died due to HIV in 2017 [1, 2]. To combat the epidemic, the Joint United Nations Program on HIV/AIDS (UNAIDS) Fast-Track strategy emphasizes the need to reduce HIV-related deaths to less than 500,000 deaths worldwide by 2020 and for a 90% reduction in HIV-related deaths by 2030 [3]. Despite increased access to antiretroviral therapy in many countries in Latin America [3, 4], not all countries show substantial reduction in HIV mortality since 2000 [1, 2]. Continued efforts are needed to track progress towards meeting the UNAIDS Fast-Track goals with respect to HIV burden and mortality.

Country-level estimates of HIV mortality in Latin America are available from a variety of sources [1, 5] and estimates of mortality exist at the state level in select countries such as Brazil and Mexico [1]. Beyond this, however, detailed subnational estimates at the second administrative level in many countries in Latin America have not been made available. This lack of subnational estimates is troubling given the localized burden of HIV in urban areas and among high-risk subgroups such as sex workers and men who have sex with men (MSM) [6–9]. Additionally, inequalities in HIV burden across local geographies likely occur given that many underlying risk factors for HIV infection and death—such as poverty, incarceration, undernutrition, and distribution of health practitioners, and access to health services—vary across geographic areas and through time [10–13]. Previous studies have observed substantial within-country variation in mortality rates [14] but are limited to select countries, areas, and years [14–17].

The paucity of evidence on subnational HIV mortality is likely due to several methodological challenges associated with a granular spatial model of HIV mortality in Latin American countries. Deaths attributable to HIV are inherently small in number in areas with small populations, leading to instabilities in the number of cases per year and adding stochastic noise to direct estimates [18]. Past approaches have used Bayesian models that apply small area methods that borrow strength across age, time, and space to produce stable estimates of mortality rates in areas with a small number of deaths [15, 19–21]. However, because of stigma or misdiagnosis, in many countries HIV deaths were assigned to other underlying causes of death such as tuberculosis, endocrine disorders, meningitis, or encephalitis [22–24] and methods are needed to correct for these misclassified deaths. Moreover, vital registration (VR) systems in many countries are incomplete and not all deaths are recorded in official statistics [22, 24–26]. While a variety of methods have been proposed to estimate the completeness of death registration at

the country level [27, 28], standard methods rely on stable population and sex pattern assumptions that often do not hold in small subnational areas [28, 29]. Recently, Schmertmann and Gonzaga proposed a Bayesian model framework to address some of the challenges of small area mortality estimation in countries with incomplete VR [30]. This method incorporates a novel functional form for mortality, that is informed by prior distributions for VR completeness coverage based on empirical evidence.

In this analysis, we apply a small area estimation framework that incorporated prior information on VR completeness to produce estimates of HIV mortality and deaths due to HIV by age at the municipality level in six countries in Latin America: Brazil, Mexico, Guatemala, Costa Rica, Colombia, and Ecuador. We chose these countries based on availability of VR data mapped to subnational levels, and data availability varied by country. This modelling approach leverages information from neighboring areas across space and time to produce estimates across all years of available data. Our analysis ranges from 2000 to 2017 in Brazil, Colombia, and Mexico; from 2009 to 2017 in Guatemala; from 2004 to 2014 in Ecuador; and from 2014 to 2016 in Costa Rica.

Methods

Overview

This analysis complies with the Guidelines for Accurate and Transparent Health Estimates Reporting (GATHER) [31]. Our study provides estimates of the HIV mortality rate and the number of HIV deaths by age group, sex, and municipality for Brazil, Colombia, Costa Rica, Ecuador, Guatemala, and Mexico for all years of available VR data. All analyses were carried out at the second administrative unit level, which we refer to as municipalities for convenience unless referencing country-specific results, where we use the appropriate national nomenclature for the administrative subdivision (municipality for Brazil, Colombia, Guatemala, Mexico; canton for Costa Rica and Ecuador). Municipalities were combined as needed to create stable units of analysis over the study period, reducing the total number of areas analyzed in select countries (Table 1). In the results, all presented rates are age-standardized for comparison between countries, unless otherwise stated.

Data

Vital registration data

Vital registration (VR) mortality data consisted of anonymized individual-level records from all deaths reported in each country's VR system occurring between the years of study (table S1 in the appendix). These records were tabulated by municipality of residence, age group (0, 1–4, 5–9, 10–14, …, 75–79, and ≥80 years), sex, and the underlying cause of death according to the tenth revision of the ICD (ICD-10) [32]. We standardized VR data using methods developed for GBD [1]. This process requires all deaths to be attributed to a single underlying cause of death following ICD guidelines and fits within a hierarchy of mutually exclusive and collectively exhaustive causes. Deaths that were coded with ICD-10 codes that could not be an underlying cause of death, as well as deaths that were coded to non-specific causes of death, were redistributed to most detailed causes of death by age, sex, municipality, and year according to a framework developed by Naghavi *et al.* [33] and updated for GBD 2017 [1]. The Global Burden of Disease 2017 Study included a correction to account for the misclassification of HIV/AIDS deaths during peak epidemic years in select countries; however, this correction did not change the number of deaths assigned to HIV/AIDS at the national level in any of the countries and years included in the present study.

Location hierarchy

We created country-specific location hierarchies that list all subnational administrative units for each year in the specified time period and match each corresponding death from the VR system to the municipality level. For each country, municipalities were geo-matched to shapefiles provided by GAUL [34] (Brazil, Costa Rica, Guatemala) or the Humanitarian Data Exchange [35] (Colombia, Ecuador, Mexico). In all selected countries, municipality boundaries changed over time, reflecting new boundary designations across the years of study (Table 1). Municipalities that underwent a boundary change during the period of the analysis were merged to create a stable unit across the period of observation, and the municipality-level shapefiles were manually edited to match the split hierarchy using ArcMap [36]. Merged units that include multiple municipalities were modelled as one area, and in the results share the same estimates of HIV mortality. Details of these shifts are provided in Table S2 in the supplementary appendix.

Covariates and population

We included several available covariates to help inform estimates of HIV mortality. Covariates applied annually at the municipality level included population density [37], night-time light brightness [38], urbanicity [39], and travel time to the nearest settlement of more than 50,000 inhabitants [40] (Table S3 in the appendix). Each covariate was obtained in a raster format and required aggregation to the modelled municipality level for inclusion in our modelling framework. This aggregation was done fractionally: raster cells that crossed municipality borders were fractionally allocated to municipalities in proportion to the covered area. We created age- and sex-specific populations for each municipality unit by aggregating the WorldPop [37] raster to the modified shapefile, utilizing the same fractional aggregation process where the population of a given pixel that spanned the boundary of two or more municipalities was divided between those units based on the proportion of the pixel area that fell into each municipality. The age- and sex-specific populations for municipalities were then scaled to the national population estimates derived from GBD [1]. This resulted in age- and sex-specific population estimates for each municipality which aligned with the GBD national population sizes and structures.

Statistical model

Vital registration completeness

We use a Bayesian hierarchical modelling framework to account for VR systems that vary in completeness by municipality and over time. Our methods expand upon a similar procedure developed in Brazil [30], where a Bayesian framework bypasses a lack of identifiability between the mortality rate and completeness estimate by incorporating an informed prior on the VR completeness. In this analysis, we incorporate information from GBD [1] on subnational (for Brazil and Mexico) and national VR completeness (for remaining countries) as well as geographic patterns in under-5 VR completeness from past analyses [41] to generate priors on municipality-level VR coverage by two age groups (<15 year-old's and 15+) and year.

In the present analysis, we model different levels of VR completeness in children and adolescents under 15 years (<15) and for adults ages 15 years and over (15+). We model these age groups separately based on the available national VR completeness estimated in GBD and established literature and expert opinion [42]. We do not model VR completeness for adults if GBD completeness estimates for adults from death distribution methods (DDM) exceeds 95% in all years of available VR (Costa Rica and Colombia). Similarly, we do not model under-15 VR completeness if GBD estimates of child completeness is greater

than 90% in all years of VR data (Costa Rica, Guatemala, Mexico). We therefore model adult completeness in Ecuador, Guatemala, Mexico, and Brazil, and model child completeness in Ecuador, Colombia, and Brazil.

Underlying geographic variation in VR completeness

In order to build priors on geographic variation in VR completeness, we used the underlying geographic variation in completeness in under-5 mortality measures. We estimated VR completeness in under-5 mortality by comparing the number of under-5 deaths in each municipality from previous analyses [41], where they exist, and compare to the reported number of under-5 deaths from VR data. Previous research produced estimates of under-5 mortality in Ecuador, Colombia, Guatemala, and Costa Rica that do not rely on vital registration data and produced 1000 draws of the number of deaths at the 5 x 5-km level [41]. In these four countries, we used these estimates to generate underlying geographic variation in VR completeness. In Mexico and Brazil, we proceed with a slightly different methodology that leverages state-level estimates of completeness produced by GBD and is described below.

To generate estimates of underlying geographic variation in VR completeness in Ecuador, Colombia, Guatemala, and Costa Rica, we first aggregated estimates of under-5 mortality from the 5 x 5-km grid cell level to each municipality at the draw level by year, such that we derived 100 draws of the number of under-5 deaths in each area j and year t. We aggregated these estimates by intersecting each grid cell with the municipality-level shapefile to determine what fraction of the area of each grid cell fell within each municipality. For cells split across multiple units, we allocated the number of under-5 deaths in proportion to area. These estimates denote the expected number of deaths in the under-5 age group used to inform the denominator for our initial VR completeness estimates π_j^*.

We use the number of reported VR deaths in each area for children under 5 as the numerator for our initial VR completeness estimates π_j^*. Due to stochastic variation from year to year in the total number of deaths by area, especially in areas with low child populations, we aggregated VR deaths over all reported years to smooth the number of deaths over time. Nonetheless, after combining child VR deaths across all years in a given area, in some countries there are still areas that report zero deaths. Given that we do not believe completeness is zero in these areas and this likely represents stochastic noise, we used a spatial smoothing model to derive more robust estimates of reported under-5 deaths. The spatial smoothing model is outlined below:

$$d_j \sim \text{Poisson}\left(E_j e^{\beta_0 + s_j + \epsilon_j}\right)$$

$$\epsilon_j \sim \text{N}(0,\ \sigma_\varepsilon^2)$$

$$S_j \sim \text{ICAR}(0,\ \sigma_S^2)$$

The model was fit in R-INLA[43] using the BYM2[44] model to "borrow strength" from the geographic pattern in reported VR deaths while still allowing for non-spatially structured variation. We used first-order queen contiguity of the spatial units to form the graph for the spatial model. We chose this model over the classic BYM model because it parameterizes the relationship between the spatially structured random effect S_j and the unstructured random effect ϵ_j in terms of two hyperparameters: τ which is the marginal precision and φ which is the portion of the marginal variance described by the spatially structured random effect. This change improves the interpretability of the hyperparameters. We used the uninformative default penalized complexity priors[44, 45] available in INLA for these hyperparameters:

$$\varphi = PC(0.5, 0.5)$$
$$\tau = PC(1, 0.01)$$

In the first case, this prior indicates a 50% probability that 50% or more of the variation is spatially autocorrelated. In the second, this prior indicates a 1% chance that the log precision is less than 1. After fitting the model, we calculate the smoothed number of VR under-5 deaths by using the mean estimate of the mortality rate for each area j and multiplying by the sum of the under-5 population over all years. We produce 1000 draws (i) of the underlying completeness π^* for each area j:

$$\pi^*_{j,i} = \text{VR deaths}_j \Big/ U5M\ deaths_{j,i}$$

There are certain areas where $VR\ death_j > U5M\ deaths_{j,i}$ and completeness estimates are above 1. Given that we have no reason to believe certain areas are overreporting deaths, we truncated completeness to either the 99th percentile of completeness draws in that municipality or 0.99, whichever is greater.

Calibrating to national VR completeness by age group

The methods outlined above produced estimates of the subnational geographic variation in VR completeness by municipality in Ecuador, Colombia, Guatemala, and Costa Rica, but this variation is not specific to year or age group. We proceed with two different frameworks, one for adult VR completeness estimates and one for child completeness estimates. For both under-15 and adults, we rescale the municipality-level completeness estimates such that the death-weighted aggregation matches the GBD national VR completeness estimates.

For national adult VR completeness, GBD produces 1000 draws (i) of completeness for each country and year t, $\Pi_{t,i}$. We rescale our initial estimates of municipality-level VR completeness, $\pi^*_{j,i}$, at the draw level such that the expected number of true deaths among adults in each area j and year t, calculated as the number of reported adult VR deaths $d^{adult}_{j,t}$ divided by completeness $\pi^*_{j,i}$ is equal to the total number of expected national deaths by year D^{adult}_t. The total number of expected national deaths D^{adult}_t is calculated as the sum of all area-level adult VR deaths $D^{adult}_t = \sum_j d^{adult}_{j,t}$ divided by the national GBD completeness $\Pi_{t,i}$. We rescale the municipality-level completeness estimates at the draw level in logit space to ensure completeness remains between zero and one while scaling the expected number of deaths to GBD by adding an adjustment factor $c^{adult}_{t,i}$ as represented in the equation below for each country:

$$\sum_j \left(d^{adult}_{j,t} \Big/ \text{logit}^{-1}(\text{logit}(\pi^*_{j,i} + c^{adult}_{t,i})) \right) = D^{adult}_t \Big/ \Pi_{t,i}$$

$$\sum_j d^{adult}_{j,t} = D^{adult}_t$$

We calculated and applied 1000 draws of the adjustment factor $c^{adult}_{t,i}$ to each municipality-draw of the initial completeness in year t to produce 1000 draws of initial completeness for each municipality and year: $\pi^{\text{adult}}_{j,t,i} = \text{logit}^{-1}(\text{logit}(\pi^*_{j,i} + c^{adult}_{t,i}))$.

For child VR completeness, we undertook a different approach given that GBD does not produce draw of child completeness from DDM methods. In this case, for each country and year t we pulled 1000 draws of the estimated under-15 all-cause deaths from the GBD, $D^{under15}_t$. We then rescaled the expected number under-15 deaths in an area j and year t to equal to the estimated number of under-15 deaths from GBD by applying an adjustment factor $c^{under15}_{t,i}$ to each municipality in logit space:

$$\sum_j d^{under15}_{j,t} \Big/ \text{logit}^{-1}(\text{logit}(\pi^*_{j,i} + c^{under15}_{t,i})) = D^{under15}_{t,i}$$

We calculated and applied 1000 draws of the adjustment factor $c^{under15}_{t,i}$ to each municipality-draw of the initial completeness in year t to produce 1000 draws of initial completeness for each municipality and year: $\pi^{\text{under15}}_{j,t,i} = \text{logit}^{-1}(\text{logit}(\pi^*_{j,i} + c^{under15`}_{t,i}))$.

Completeness draws for Brazil and Mexico

For Brazil and Mexico, we leverage state-level estimates of VR completeness for adults and children produced by GBD[1]. For state-level adult VR completeness, GBD produces 1000 draws (i) of

completeness for each state J and year t, $\Pi_{J,t,i}$.These estimates of adult completeness at the state level are modelled directly in our small area estimation framework, where each municipality that nests within a state is assumed to follow the same prior and contributes to the same posterior level of VR completeness.

For under-15 completeness in Brazil, given that GBD does not produce draw level completeness, we pull 1000 draws of estimated under-15 all-cause deaths for each state J and year t: $D_{J,t,i}$. We then calculate draws of completeness by taking the ratio of the reported all-cause deaths for each state J and year t from VR data and $D_{J,t,i}$:

$$\pi_{J,t,i}^{\text{under15}} = {VR\ deaths_{J,t}}\Big/{D_{J,t,i}}$$

In a small number of state draws, completeness estimates are greater than 1 and these are truncated to 0.99. These estimates of under-15 completeness at the state level are modelled directly in our small area estimation framework, where each municipality that nests within a state inherits the same prior and contributes to the posterior for VR completeness.

Prior specification

The processes outlined above generate draws of both adult and under-15 completeness for each municipality (Ecuador, Colombia, Guatemala, and Costa Rica) or state (Brazil and Mexico) by year. To include these informed priors in our modelling framework, we characterized the distribution by fitting to a logit-normal distribution using maximum likelihood estimation. For area-municipality-years where all draws were truncated at 0.99, we fit the model with a mean of 0.99 and a standard deviation of 0.01 in logit space.

Statistical models

We fit the following hierarchical generalized linear model for VR data, building on a model developed in prior modelling studies[15, 46]

$$\begin{aligned}
D_{j,t,a} &\sim \text{Poisson}\left(m_{j,t,a} \cdot \pi_{k,t,a^*} \cdot P_{j,t,a}\right) \\
\log\left(m_{j,t,a}\right) &= \beta_0 + \beta_1 \cdot X_j + \gamma_{1,a,t} + \gamma_{2,j} + \gamma_{3,j} \cdot \text{t} + \gamma_{4,j} \cdot \text{a} + \gamma_{5,j,t} + \gamma_{6,j,a} \\
\gamma_{1,a,t} &\sim \text{LCAR: LCAR}\left(\sigma_1^2, \rho_{1,A}, \rho_{1,T}\right) \\
\gamma_{2,j} &\sim \text{LCAR}(\sigma_2^2, \rho_2) \\
\gamma_{3,j} &\sim \text{LCAR}(\sigma_3^2, \rho_3) \\
\gamma_{4,j} &\sim \text{LCAR}(\sigma_4^2, \rho_4) \\
\gamma_{5,j,t} &\sim \text{N}\left(0, \sigma_5^2\right)
\end{aligned}$$

$$\gamma_{6,j,a} \sim \mathrm{N}(0, \sigma_6^2)$$

$$1/\sigma_i^2 \sim \mathrm{Gamma}(1, 1000) \text{ for } i \in 1, 2, 3, 4, 5, 6$$

$$\mathrm{logit}(\rho_i) \sim \mathrm{Normal}(0, 1.5) \text{ for } i \in 1A, 1T, 2, 3, 4$$

where $D_{j,t,a}$ represents the number of HIV deaths in municipality *j*, year *t,* and age group *a;* $m_{j,t,a}$ is the mortality rate in municipality *j*, year *t,* and age group *a*; π_{k,t,a^*} is the VR completeness in municipality (Ecuador, Colombia, Guatemala, and Costa Rica) or state (Brazil and Mexico) *j*, year *t,* and completeness age group a^* (<15, 15+); $P_{j,t,a}$ is the population in municipality *j*, year *t,* and age group *a*; β_0 is the intercept; $\beta_1 \cdot X_j$ is the vector of covariates and associated regression coefficients; $\gamma_{1,a,t}$ describes the overall age-time pattern; $\gamma_{2,j}$ describes spatial patterns that persist over age and time, $\gamma_{3,j} \cdot \mathrm{t}$ describes area-specific deviations from the overall time pattern; $\gamma_{4,j} \cdot \mathrm{a}$ describes area-specific deviations from the overall age pattern; $\gamma_{5,j,t}$ and $\gamma_{6,j,a}$ allow for area-specific non-linear deviations from the overall time and age patterns, respectively.

VR completeness is incorporated into the data generating model, and logit-normal priors on π_{k,t,a^*} fit on empirical data as described above allow the model to distinguish between mortality rate $m_{j,t,a}$ and the VR completeness. Random effects $\gamma_{1,a,t}, \gamma_{2,j}, \gamma_{3,j}, \gamma_{4,j}$ were assigned a Leroux conditional autoregressive prior (LCAR) [47]. The full conditional distribution can be described by:

$$\gamma_i | \gamma_{k\sim i}, \sigma^2, \rho \sim \mathrm{Normal}\left(\frac{\rho \sum_{k\sim i} \gamma_k}{n_i \cdot \rho + 1 - \rho}, \frac{\sigma^2}{n_i \cdot \rho + 1 - \rho}\right)$$

where: $k \sim i$ denotes the set of I's "neighbors" (for spatial terms, municipalities that share a border; for temporal/age terms, adjacent years/age groups); n_j is the number of neighbors in $k \sim i$; σ^2 is the variance parameter; and ρ is the correlation parameter. These random effects allow for additional variation across space, time, and age that is not explained by the covariates. For each of the random effects, the variance (σ^2) denotes the amount of variation, while the correlation (ρ) determines how much smoothing takes place, ρ ranged 0 to 1 with higher values indicating greater spatial smoothness. We assigned Gamma(0, 1000) hyperpriors for the precision of each random effect and Normal(0, 1.5) hyperpriors for the logit-transform of the correlation parameters. The random effects $\gamma_{5,j,t}$ and $\gamma_{6,j,a}$ were assumed to follow independent mean-zero normal distributions.

We model γ_1 as an interaction between two conditional autoregressive (LCAR) distributions as defined above for age and time, respectively. This was specified according to the procedure described by

Knorr-Held[48] (i.e., a 'Type IV' interaction). This specification allows for smoothing over age group and time simultaneously, such that the level for a given age group and year is informed both by first-order neighbors (i.e., adjacent years in the same age group and adjacent age groups in the same year) as well as second order neighbors (i.e., adjacent years in adjacent age groups). For this distribution there are three hyperparameters: σ^2, which control the overall amount of variation, and $\rho_{1,A}$ and $\rho_{1,T}$ which control the smoothness over age and time, respectively.

Models were estimated separately for each country and sex and fit using the TMB package [49]. One thousand draws were sampled from the approximated posterior distributions of each modelled parameter and used to construct 1000 draws of $m_{j,t,a}$. We calculated point estimates from the mean of these draws, and the lower and upper bounds of the 95% uncertainty interval from the 2.5th and 97.5th percentiles, respectively, for each age, sex, year, and municipality. Municipality-level estimates for each cause and sex were aggregated to the state and national level using a population-weighted average. In Brazil and Mexico, estimates were calibrated to GBD at the state level and estimates were calibrated to national HIV mortality estimates for the remaining four countries. For each year t and age group a, we calculated the ratio of the national- or state-level estimate from GBD to the mean national estimate derived from population-weighting $m_{j,t,a}$, and multiplied all draws of $m_{j,t,a}$ by this ratio. We generated the number of HIV deaths for each age-sex-year-municipality by multiplying the mean, lower, and upper bounds of our mortality estimates by the corresponding WorldPop population estimate. Throughout our analysis, we qualify statements as statistically significant if the posterior probability of that statement exceeds 95%. We completed our analysis using R version 3.6.3 [50].

Model Validation

To assess if including prior VR completeness in our statistical framework improved model estimates, for the five countries where we applied completeness priors to either children under-15 or adults we also fit a model where the completeness term in the statistical model, π_{k,t,a^*}, was removed ('standard'). We then compared the ratio of annual national HIV mortality in children under-15 and adults from GBD to 1,000 draws of national estimates of annual HIV mortality from the standard and completeness models. This ratio, known as the raking factor, is plotted in extended figures S1-S6 in the appendix. A raking factor closer to 1 indicates better alignment with GBD, and inclusion of completeness priors generally resulted in closer alignment with national GBD mortality estimates.

Results

Geographic patterns in HIV mortality and notable time trends

In Brazil, the estimated national HIV mortality rate for both sexes combined in 2017 was 6.5 (95% uncertainty interval: 6.4–6.7) deaths per 100,000 (8.7 [8.5–8.9] deaths among men, and 4.5 [4.4–4.6] deaths among women). Estimated HIV mortality for men varied over 50-fold among municipalities: from 0.9 (0.2–2.9) deaths per 100,000 in the Jordão municipality to 47.8 (36.4–61.3) deaths per 100,000 in the Tramandaí municipality (Figure 1 and Figure S7 in the appendix). Estimated female HIV mortality in 2017 ranged from 0.8 (0.3–1.7) deaths per 100,000 in the Maraa municipality to 28.6 (20.7–37.7) deaths per 100,000 in the Tramandaí municipality. Between 2000 and 2017, estimated national HIV mortality decreased by 25.3% (from 11.7 [11.4–11.9] deaths per 100,000 in 2000) in men and 14.9% (from 5.3 [5.1–5.4] deaths per 100,000 in 2000) in women. These national decreases hide substantial variation at the municipality level. Estimated male HIV mortality decreased in 3389 (60.8%) municipalities, and 91 [1.6%] municipalities had a statistically significant decrease in HIV mortality. Estimated female HIV mortality decreased in 3000 (53.9%) municipalities and 37 [0.7%] municipalities had a statistically significant decrease in HIV mortality. Changes in estimated male HIV mortality at the municipality level ranged from a 248.1% increase in Bacabal municipality (from 7.2 [4.9–10.5] deaths per 100,000 in 2000 to 25.1 [18.9–33.2] deaths per 100,000 in 2017) to a 70.9% decrease in Ribeirao Preto municipality (from 32.6 [28.6–36.9] deaths per 100,000 in 2000 to 9.5 [8.1–11.2] deaths per 100,000 in 2017). Changes in estimated HIV mortality in women at the municipality level varied from a 233.9% increase in Novo Hamburgo municipality (from 5.2 [3.9–6.9] deaths per 100,000 in 2000 to 17.4 [13.8–21.7] deaths per 100,000 in 2017) to a 68.8% decrease in Jundiai municipality (from 5.7 [4.4–7.4] deaths per 100,000 in 2000 to 1.8 [1.2–2.5] deaths per 100,000 in 2017).

In 2017, Colombia's estimated national HIV mortality rate for both sexes combined was 5.1 (4.8–5.3) deaths per 100,000 (7.8 [7.5–8.1] deaths for men, and 2.5 [2.3–2.7] deaths for women). Estimated male HIV mortality in 2017 varied over 70-fold: from 0.5 (0.2–0.9) deaths per 100,000 in the La Calera municipality to 37.6 (26.4–50.9) deaths in the Chinchiná municipality (Figure 2 and Figure S8 in the appendix). In women, estimated mortality fluctuated from 0.2 (0.1–0.5) deaths per 100,000 in the La Calera municipality to 17.2 (10.6–27.4) deaths in the La Virginia municipality. From 2000 to 2017, changes in national HIV mortality diverged by sex: estimated HIV mortality decreased in men by 19.8% (from 9.8 [9.3–10.2] deaths per 100,000 in 2000) but increased in women by 19.5% (from 2.1 [1.9–2.3] deaths per 100,000 in 2000). While national estimated HIV prevalence decreased in men and not women, HIV

mortality increased in a majority of municipalities from 2000 to 2017 in both sexes. Estimated male HIV mortality increased in 594 (52.9%) municipalities, and five (0.4%) municipalities had a statistically significant increase in HIV mortality. Estimated female HIV mortality increased in 1081 (96.3%) municipalities and five (0.4%) municipalities had a statistically significant increase in HIV mortality. There was large variation in subnational changes in HIV mortality: male estimated HIV mortality ranged from a 361.7% increase in San Andrés de Tumaco municipality (from 2.8 [1.7–4.3] deaths per 100,000 in 2000 to 12.8 [9.4–17.1] deaths per 100,000 in 2017) to a 59.7% decrease in Barbosa municipality (from 15.5 [9.4–24.5] deaths per 100,000 in 2000 to 6.2 [3.2–10.5] deaths per 100,000 in 2017). In women, estimated relative change in HIV mortality at the municipality level varied from a 170% increase in Puerto Colombia municipality (from 3 [1.5–5.4] deaths per 100,000 in 2000 to 8.2 [3.9–16.1] deaths per 100,000 in 2017) to a 31.2% decrease in Bogota, D.C. municipality (from 1.6 [1.4–1.9] deaths per 100,000 in 2000 to 1.1 [0.9–1.3] deaths per 100,000 in 2017).

Among the six countries considered, Costa Rica had the lowest HIV mortality rates in the latest year of study, with an estimated national HIV mortality rate for both sexes combined in 2016 of 3.2 (2.6–3.9) deaths per 100,000 (4.9 [4.2–5.8] deaths for men, and 1.5 [1.1–2.3] deaths for women). At the canton level, we estimated male HIV mortality varied over 100-fold in 2016, from 0.5 (0.01–2.9) deaths per 100,000 in the Aserrí canton to 52.1 (42.1–63.2) deaths in the San José canton (Figure 3 and Figure S9 in the appendix). For women, mortality ranged over 40-fold, from 0.2 (0–1.5) deaths per 100,000 in the Atenas canton to 11.9 (7.8–17.4) deaths per 100,000 in the San José canton. Between 2014 and 2016, estimated national HIV mortality decreased by 18.5% in men (from 6 [5.1–7.1] deaths per 100,000 in 2014) and by 20% in women (from 1.9 [1.4–2.7] deaths per 100,000 in 2014). Estimated HIV mortality decreased in 80 (98.8%) municipalities for men and all 81 municipalities for women, though no municipality for either sex registered a statistically significant decrease in HIV mortality. National temporal decreases were largely driven by the San José canton, which had the highest decrease in estimated male HIV mortality: 21.1%, from 65.9 [53.6–81.5] deaths per 100,000 in 2014 to 52.1 [42.1–63.2] deaths per 100,000 in 2016. From 2014 to 2016, estimated HIV mortality in San José canton decreased among women by 22.7% (from 15.3 [10.4–22.9] deaths per 100,000 in 2014 to 11.9 [7.8–17.4] deaths per 100,000 in 2016).

In 2014, Ecuador had the highest estimated national HIV mortality rate for both sexes combined among the six countries investigated: 7.0 (6.5–7.6) deaths per 100,000 (10.9 [10.1–11.7] deaths for men, and 3.4 [3.0–3.8] deaths for women). Male estimated HIV mortality varied among cantons from 1.1 (0.4–2.4) deaths per 100,000 in the Tulcán canton to 50.7 (29.0–81.6) deaths per 100,000 in the Palestina

canton (Figure 4 and Figure S10 in the appendix). For women, estimated HIV mortality ranged from 0.6 (0.2–1.3) deaths per 100,000 in the Tulcán canton to 13 (4.3–29.8) deaths per 100,000 in the San Lorenzo canton. Between 2004 and 2014, estimated national HIV mortality increased by 28.3% in men (from 8.5 [7.8–9.2] deaths per 100,000 in 2004) and increased by 63.2% in women (from 2.1 [1.8–2.4] deaths per 100,000 in 2004). Estimated male HIV mortality increased in 216 (96.4%) municipalities, and three [1.3%] municipalities had a significant increase in HIV mortality (posterior probability >95%). Estimated female HIV mortality increased in 223 (99.6%) municipalities and one [0.4%] municipality had a statistically significant increase in HIV mortality. Among men, estimated change in HIV mortality at the canton level ranged from a 239.7% increase in Río Verde municipality (from 9.1 [2.9–24.4] deaths per 100,000 in 2004 to 31 [9.5–79.1] deaths per 100,000 in 2014) to a 42.7% decrease in Huaquillas canton (from 8.3 [3.9–15.9] deaths per 100,000 in 2004 to 4.7 [1.8–10] deaths per 100,000 in 2014). Among women, estimated relative change in HIV mortality at the canton level varied from a 199.9% increase in Río Verde municipality (from 3.4 [0.9–10.2] deaths per 100,000 in 2004 to 10.2 [1.7–34.6] deaths per 100,000 in 2014) to essentially no change in Latacunga canton (0.6 [0.3–1.2] deaths per 100,000 in 2004 compared to 0.6 [0.3–1.3] deaths per 100,000 in 2014).

In Guatemala, estimated national HIV mortality for both sexes combined in 2017 was 4.6 (4.1–5.1) deaths per 100,000 (6.8 [6.2–7.4] deaths for men and 2.8 [2.4–3.1] deaths for women). At the municipality level, estimated HIV mortality for men varied from 0.8 (0.2–2.1) deaths per 100,000 in the Santa Cruz Barillas municipality to 38.6 (24.5–57.5) deaths per 100,000 in the San José municipality (Figure 5 and Figure S11 in the appendix). For women, estimated HIV mortality ranged from 0.7 (0.2–1.5) deaths per 100,000 in the Chiantla municipality to 20.3 (12.3–31.8) deaths per 100,000 in the San José municipality. Between 2009 and 2017, estimated national HIV mortality decreased by 36.9% in men (from 10.8 [9.9–11.7] deaths per 100,000 in 2009) and by 33.5% in women (from 4.1 [3.7–4.6] deaths per 100,000 in 2009). Unlike in the other countries considered, estimated HIV mortality decreased in all 340 municipalities for both sexes, though only two [0.6%] municipalities for men and no municipalities for women had a statistically significant decrease in HIV mortality. In men, estimated relative change in HIV mortality at the municipality level ranged from a 14.4% decrease in San José municipality (from 45 [30.2–65.5] deaths per 100,000 in 2009 to 38.6 [24.5–57.5] deaths per 100,000 in 2017) to a 54% decrease in Siquinalá municipality (from 25.4 [14.3–41.3] deaths per 100,000 in 2009 to 11.7 [6.5–19.7] deaths per 100,000 in 2017). Estimated change in female HIV mortality at the municipality level varied from an 18.5% decrease in San José municipality (from 24.9 [15.9–38.6] deaths per 100,000 in 2009 to 20.3 [12.3–

31.8] deaths per 100,000 in 2017) to a 39.9% decrease in Coatepeque municipality (from 6.9 [4.4–10.3] deaths per 100,000 in 2009 to 4.1 [2.6–6.6] deaths per 100,000 in 2017).

In Mexico, the estimated national HIV mortality rate for both sexes combined in 2017 was 4.3 (4.2–4.4) deaths per 100,000 (6.9 [6.7–7.1] deaths per 100,000 for men, and 1.9 [1.8–2.0] for women). At the municipality level, estimated HIV mortality for men in 2017 varied over 50-fold: from 0.8 (0.4–1.3) deaths per 100,000 in the Atenco municipality to 42.6 (29.1–61.4) deaths in the Tlacotalpan municipality (Figure 6 and Figure S12 in the appendix). For women, estimated HIV mortality ranged over 45-fold from 0.3 (0.2–0.6) deaths per 100,000 in the Texcoco municipality to 14.2 (8.8–22.0) deaths per 100,000 in the San Juan Cancuc municipality. Between 2000 and 2017, estimated national HIV mortality decreased by 23.5% in men (from 9.0 [8.8–9.3] deaths per 100,000 in 2000) and by 5.2% in women (from 2.0 [1.9–2.1] deaths per 100,000 in 2000). Estimated male HIV mortality decreased in 2048 (83.3%) municipalities, and 32 [1.3%] municipalities had a statistically significant decrease in HIV mortality (posterior probability >95%). Estimated female HIV mortality decreased in 1683 (68.5%) municipalities and 4 [0.2%] municipalities had a significant decrease in HIV mortality (posterior probability >95%). In men, estimated change in HIV mortality from 2000 to 2017 ranged from a 162.4% increase in the Solidaridad and Tulum municipalities (from 6.8 [4.9–9.3] deaths per 100,000 in 2000 to 17.9, [14.5–21.6] deaths per 100,000 in 2017) to a 61.9% decrease in Playas de Rosarito municipality (from 19.3 [13.6–27.2] deaths per 100,000 in 2000 to 7.4 [5.1–10.2] deaths per 100,000 in 2017). For women, estimated relative change in HIV mortality at the municipality level varied from a 110.3% increase in Coatzacoalcos municipality (from 4.5 [3.5–5.8] deaths per 100,000 in 2000 to 9.5 [7.5–11.8] deaths per 100,000 in 2017) to a 54.9% decrease in Zapopan municipality (from 2.5 [1.9–3.3] deaths per 100,000 in 2000 to 1.1 [0.8–1.5] deaths per 100,000 in 2017).

Absolute and relative inequality over time

Figure 7 depicts the relative and absolute inequality over time in each country. Relative inequality, quantified here as the mortality rate ratios for municipalities in the 90th percentile versus those in the 10th percentile, varied from 5.0 (4.9–5.2) and 4.8 (4.6–5.0) among men and women in Brazil in 2017, to 63.4 (31.6–113.0) and 167.6 (54.6–403.5) among men and women in Costa Rica in 2016. The estimated relative geographic inequality in HIV mortality increased in all countries from the first to the last year of study, and this increase was statistically significant, in all countries barring Guatemala and Costa Rica. The largest percent increase in relative inequality for each sex over the study period was 49% in Colombian

men (from 6.5 [6.0–7.0] in 2000 to 9.6 [8.8–10.5] in 2017) and 55.9% in Ecuadorian women (from 4.7 [4.0–5.5] in 2004 to 7.4 [6.1–8.8] in 2014).

Absolute inequality, quantified here as the difference between the mortality rate in the 90th percentile and the 10th percentile, showed less temporal variation in Brazil, Mexico, and Costa Rica: the difference in estimated absolute inequality between the first and last year of study was less than 1.5 deaths per 100,000 among both men and women. Male absolute inequality increased in Colombia by 40.9% (from 6.9 [6.4–7.4] in 2000 to 9.7 [9.1–10.4] in 2017) and in Ecuador by 74.1% (from 13.5 [11.8–15.4] in 2004 to 23.6 [21.0–26.4] in 2014), while male absolute inequality decreased in Guatemala by 48.2% (from 17.8 [15.8–19.8] in 2009 to 9.2 [8.1–10.4] in 2017). Female absolute inequality increased in Colombia by 50.8% (from 2.2 [2.0–2.4] in 2000 to 3.3 [3.0–3.6] in 2017) and Ecuador by 123.9% (from 3.6 [3.0–4.3] in 2004 to 8.1 [6.8–9.6] in 2014), while female absolute inequality decreased in Guatemala by 43.5% (from 6.2 [5.4–7.2] in 2009 to 3.5 [3.0–4.1] in 2017). For both men and women, increases in absolute relative inequality in Colombia and Ecuador, as well as decreases in absolute inequality in Guatemala, were statistically significant.

Local disparities in median age group among those who died from HIV

Figure 8 shows the estimated median age group of men and women who died from HIV by municipality. Estimated median age group among men who died in the latest year of study varied at the municipality level by 15 years in Brazil, Ecuador, and Mexico, and by ten years in Colombia, Costa Rica, and Guatemala. Among women, estimated median age group among those who died in the latest year of study varied at the municipality level by 15 years in Brazil, Guatemala, and Mexico, by ten years in Colombia, and by only five years in Costa Rica and Ecuador. Differences in median age group among those who died also shifted over time. In Brazil, the estimated median age group among male decedents rose in 99.6% of municipalities from 2000 to 2017, while in Guatemala only 21.5% of municipalities saw an increase in estimated median age group among male decedents from 2009 to 2017. An increase in estimated median age was also observed among women: in Mexico, Ecuador, Colombia, and Brazil the median age group among female decedents rose in >97% of all municipalities in each country. Figures S13-S18 in the appendix show estimated HIV mortality by age group and sex for each country in the last year of study.

Concentrated deaths due to HIV

We estimated that a large proportion of HIV deaths were concentrated in a small number of geographical areas with large populations (Figure 9). In all countries, over half of the HIV deaths were located in less than 10% of municipalities in the latest year of study. In Colombia, over half of all HIV deaths in 2017 were located in just 1.2% (14 of 1122) of municipalities that contain 37.0% of the total population; and in Guatemala in 2017 over half the HIV deaths were spread out over 9.4% (32 of 340) of municipalities that contain 33.4% of the population. Several countries contained single municipalities that contributed a large proportion of national HIV deaths: for example, in Costa Rica in 2016, 45.9% of all HIV deaths were located in San José canton compared to 4.6% of the total population. Mexico had a greater spread of HIV deaths across municipalities; in 2017 the area with the highest proportion of HIV deaths was Tijuana municipality which amounted to 3.2% of the total deaths compared to 2.5% of the population. There was higher HIV mortality in men as compared to women in all countries, ranging from 64.7% of all deaths concentrated in men in Brazil in 2017, to 77.6% of all deaths concentrated in men in Mexico in 2017.

Discussion

There are few past analyses that assess HIV mortality in Latin America using vital registration data at a subnational level, largely due to the statistical challenges of incorporating incomplete VR systems and estimating mortality in areas with small numbers of deaths. The few analyses that integrate estimates of VR completeness into their modelling framework are often done at the national or state level or are limited to a single country and year [14–17]. In this analysis, we expand on previously described methods that include prior estimates of VR completeness and demonstrate the utility of estimates that combine uncertainty from both incomplete registration systems and from statistical methods designed to leverage information across space, time, and age to inform mortality rates in areas with small numbers of HIV deaths.

Our estimates revealed large-scale spatial heterogeneity in HIV mortality across the six Latin American countries considered in our analysis. We also reveal divergent national trends in HIV mortality in the six countries across the study period, and variable relative change within countries at the municipality level. From the first to the last year of study, HIV mortality decreased among men and women in all countries, with the exception of women in Colombia from 2000 to 2017 and both men and women in Ecuador from 2004 to 2014. Despite the progress in reducing HIV mortality among both sexes at the national level in Brazil, Guatemala, Costa Rica, and Mexico, inequalities in municipality-level HIV

mortality persist. Relative inequality, or the mortality rate ratio between the municipalities in the 90th and 10th percentile, increased over time in all countries. This analysis highlights uneven progress towards reducing HIV mortality and reaching UNAIDS Fast-Track goals, and emphasizes an alarming trend in Ecuador, where over 95% of cantons increased in estimated mortality among both sexes from 2004 to 2014. Nonetheless, it also underlines stories of success: all countries registered municipalities with an estimated decrease in HIV mortality. Further evaluating municipalities with the greatest decreases in HIV mortality within a country may help decision-makers recognize successful strategies that could be implemented in municipalities experiencing increases or slower declines.

There are likely a multitude of factors that contribute to the spatial and temporal patterns in HIV mortality observed in our analysis. Consistent with past analyses, we found higher rates of HIV mortality in men compared to women and slightly different spatial patterns by sex [15, 51, 52]. The consistently elevated levels of mortality among men is likely because men who have sex with men (MSM) continue to be one of the populations with the highest prevalence throughout Latin America, and a group that suffers a higher level of stigma and discrimination [51, 53]. These trends may also reflect prevalent gender norms [52], or unequal access by gender to timely diagnosis and treatment [51]. The spatial distribution of high-risk groups possibly also contributes to the HIV epidemic remaining concentrated in large urban centres [6]. Another important driver of spatial differences in HIV mortality is prison populations, where HIV transmission is high due to overcrowding, violence, and lack of information on the risk of HIV acquisition [54]. In Brazil, there is evidence of low adherence to ART and a higher proportion of primary and secondary resistance among prison populations, which are predominantly male [55]. Municipalities with large prison populations—such as several in the state of Sao Paulo, Brazil—show higher levels of HIV mortality rates and number of deaths due to HIV. A key driver of temporal trends in HIV mortality is the implementation of ART treatment programs, which has been incorporated in all Latin American countries and led to impressive increases in ART coverage [56]. In 2017, universal access to ART coverage was rolled out in all countries and studies have documented the resulting decreases in HIV mortality [57]. Nonetheless, persistent differences in access and adherence to ART remain [6] and may contribute to differences in HIV mortality declines observed in this analysis.

Our analysis also revealed substantial variation in median age group among those who died from HIV at the municipality level, and an increase over time in median age group among those who died of HIV. These results agree with past research that demonstrates an accelerating growth in the number of people living with HIV that are above 50 years of age [58]. Several countries, notably Brazil and Mexico, contained municipalities with a 15-year difference in median age groups among men and women who

died from HIV in the latest year of study. While attributing these trends to specific drivers is outside the scope of this analysis, there are several factors that could influence an increase in median age of death, including changes in HIV incidence in specific age groups [59], increases in life expectancy among people living with HIV [59], access to ART [60], migration, and the age distribution of the population across the study period.

This analysis provides novel subnational estimates of HIV mortality that convey important information to policymakers and could inform future action. Knowledge of local differences in HIV mortality can help guide scale-up of ART where mortality might reflect suboptimal coverage. In the longer term, HIV mortality measures could be used to highlight areas that might benefit from programmatic interventions that target HIV prevention such as pre-exposure prophylaxis (PrEP). As countries in Latin America consider expanding access to PrEP, studies have demonstrated that prioritization of PrEP to those at highest risk could save money and lives [61, 62]. Cost-effective interventions are especially important in Guatemala, Ecuador, Colombia, and Costa Rica, where HIV programs depend on donor funding [63]. Furthermore, subnational differences in HIV burden have already been used to develop localized strategies for HIV prevention and elimination in sub-Saharan Africa [64, 65].

Limitations

This analysis is subject to several limitations. First, the VR data we use to inform our estimates are subject to misclassification biases. HIV is generally under-reported as a cause of death [22]. While the GBD mortality redistribution method employed in this analysis corrects for biases in HIV deaths classified to other underlying causes of death there may be additional country-specific biases not addressed by our methodological approach. Second, our method for correcting for incomplete VR across space and time makes several crucial assumptions. Our analysis incorporates estimates of VR completeness for children under 15 and adults 15 and over based on previous analyses, but VR completeness may vary within these age ranges. Further, we use the geographic variation in completeness identified by comparing reported under-5 all-cause deaths to previous estimates, and the variation in under-5 mortality may not be comparable to patterns in adult VR incompleteness. Additionally, variation in all-cause completeness may differ from patterns in HIV-specific VR completeness. Third, we use population estimates from WorldPop in this analysis that are subject to error, especially in sparsely populated areas. While WorldPop estimates include census data as inputs [66], depending on timing and data accessibility, estimates may differ from the underlying census measures and may not utilize the most recent census or the most detailed tabulations. Fourth, our analysis is subject to large uncertainty. This reflects uncertainty both due to the

small number of HIV deaths at the municipality level and the need to estimate completeness. While we believe this method better captures all sources of uncertainty, care must be taken when interpreting results. Fifth, we use custom shapefiles that are matched to country-level administrative subdivisions, and differences in administrative divisions between GAUL [34] or the Humanitarian Data Exchange [35] and an individual country's designation of administrative areas may affect the accuracy of results, especially in our estimates of the number of HIV deaths by municipality. Sixth, our small area estimation models smooth over space and time by making assumptions about the temporal and spatial structure of HIV mortality that may not always hold. Seventh, VR data availability varied across the countries selected in our analysis, and comparison between temporal trends in HIV mortality may be difficult to assess for countries with different years of data availability. Finally, it is difficult to assess the accuracy of our results, which may be adversely affected due to violations of the modelling assumptions or quality issues in the underlying data sources.

Future directions

There is considerable opportunity to expand this analysis. First, access to VR data over more years of study, or in neighbouring countries in Latin America, could provide valuable benchmarks for more direct comparisons and allow additional information across space and time to potentially improve our models. Further, the technique we used to include uncertainty and information on subnational VR completeness could be extended to other countries where VR systems are not complete. Finally, this small area estimation framework could be used to estimate all-cause and cause-specific mortality due to other causes at local levels in the six modelled Latin American countries.

Conclusion

Our analysis finds large-scale variation in HIV mortality among municipalities in the six selected Latin American countries, both in the latest year of study as well as over the entire study period. Our estimates demonstrate the need to assess HIV burden at a granular geographic scale in Latin America, given that the HIV epidemic is concentrated in high-risk groups and select urban areas. The methods further developed in this analysis provide a framework for incorporating prior information on VR completeness into subnational estimates of HIV burden. This analysis could be used to identify areas that have successfully reduced HIV mortality and areas of high HIV burden, as well as to inform the rollout of

preventive interventions that are required to help countries progress towards the UNAIDS Fast-Track goal of a 90% reduction in HIV-related deaths by 2030.

Acknowledgements

This thesis would not have been possible without many people's help. First, I would like to thank my committee chair and supervisor Dr. Laura Dwyer-Lindgren for all of her help with the manuscript and throughout my time as a master's student. Her patience, motivation, and knowledge challenged me to be a better researcher—I cannot imagine a better mentor. I would also like to thank my other committee member, Dr. Simon I. Hay, for his directive feedback and insightful comments that kept me on track.

Besides my thesis committee, I want to thank the geospatial vital registration team for their help in providing the data for this project. Thank you Nat Henry, Ian Letourneau, Stefanie Watson, Kate LeGrand, Andrew Croneberger, Mathew Baumann, and Michael Collison, for always being quick to help when something came up, you all were crucial to getting this work completed.

I also received great feedback from the Local Burden of Disease HIV team–thank you Emily Haeuser, Mingyou Yang, Audrey Serfes, and John VanderHeide for their motivation and help with the manuscript over the past months.

Lastly, I would like to thank my family, my partner, and my friends who supported me throughout my graduate studies.

Table 1: Years of study, names, and number of second administrative subdivisions by country

Country	Years of available VR data	Name of second administrative subdivision	Total number of second administrative subdivisions	Number of modelled units in this analysis
Brazil	2000–2017	Municipality	5,570	5,477
Colombia	2000–2017	Municipality	1,122	1,115
Costa Rica	2014–2016	Canton	81	81
Ecuador	2004–2014	Canton	224	222
Guatemala	2009–2017	Municipality	340	333
Mexico	2000–2017	Municipality	2,458	2,441

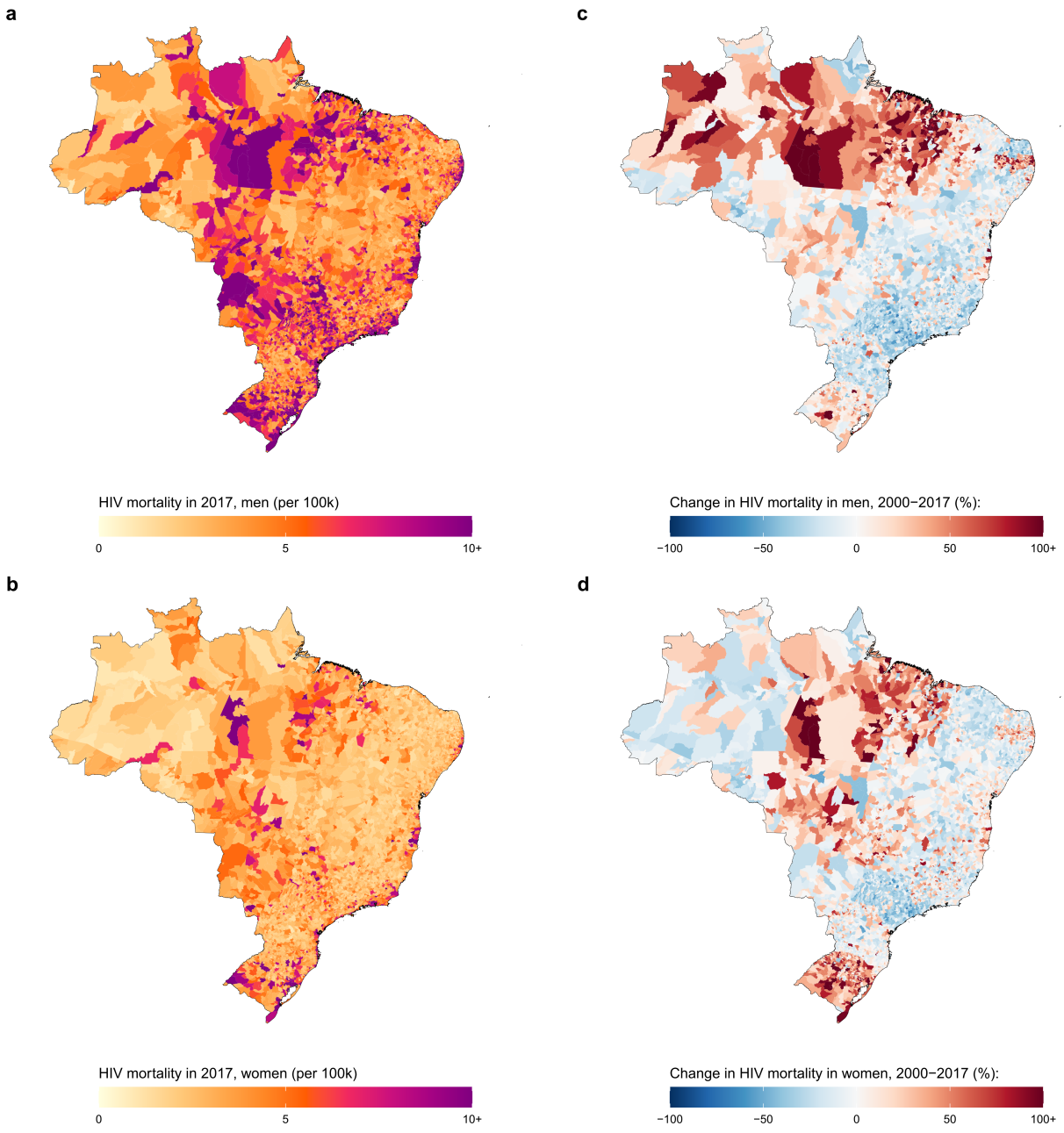

Figure 1: HIV mortality among men and women in Brazil by municipality, 2017
HIV mortality per 100,000 by municipality in Brazil in 2017 among men (a) and women (b). Relative change in HIV mortality between 2000 and 2017 among men (c) and women (d).

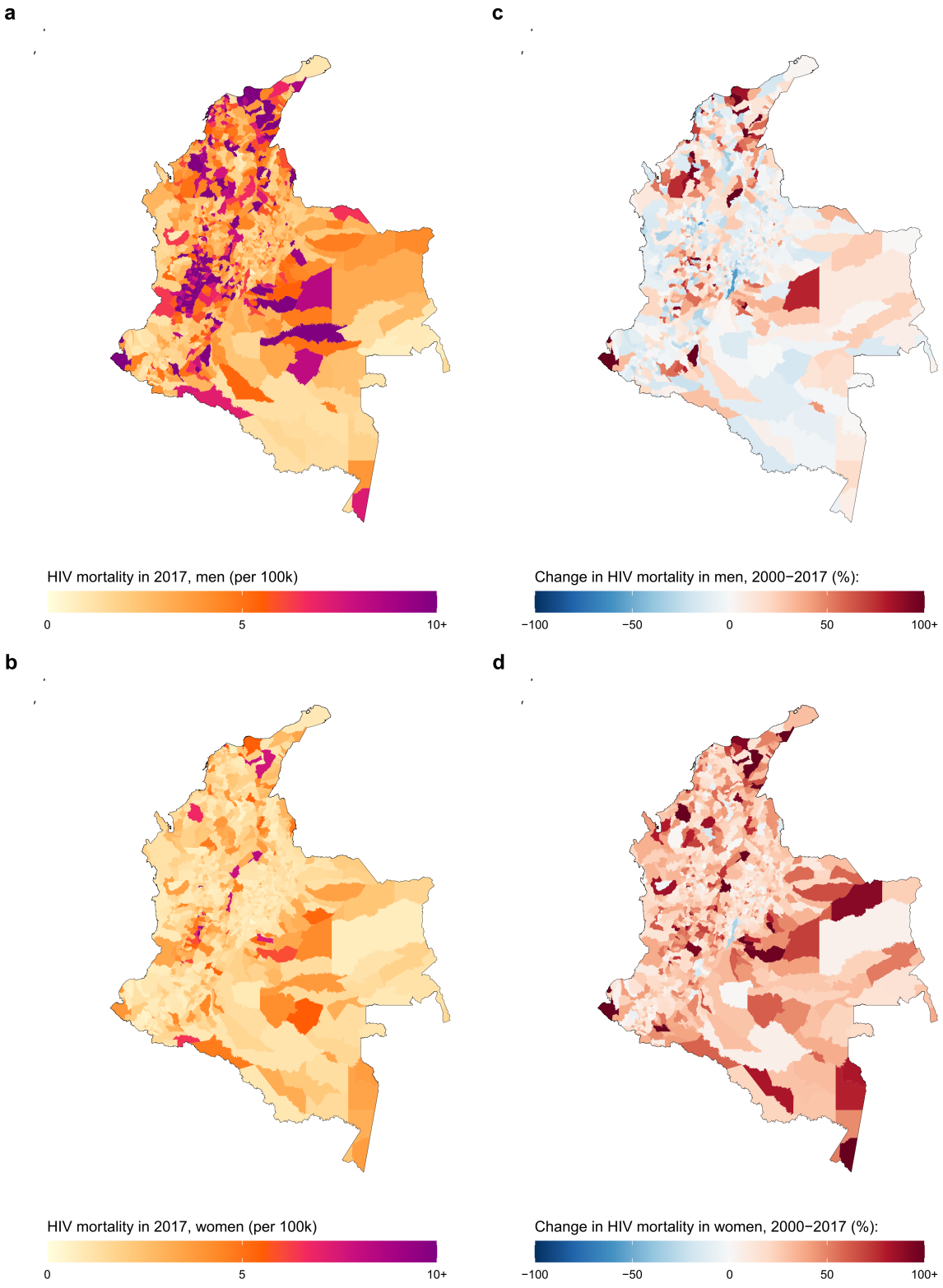

Figure 2: HIV mortality among men and women in Colombia by municipality, 2017

HIV mortality per 100,000 by municipality in Colombia in 2017 among men (a) and women (b). Relative change in HIV mortality between 2000 and 2017 among men (c) and women (d).

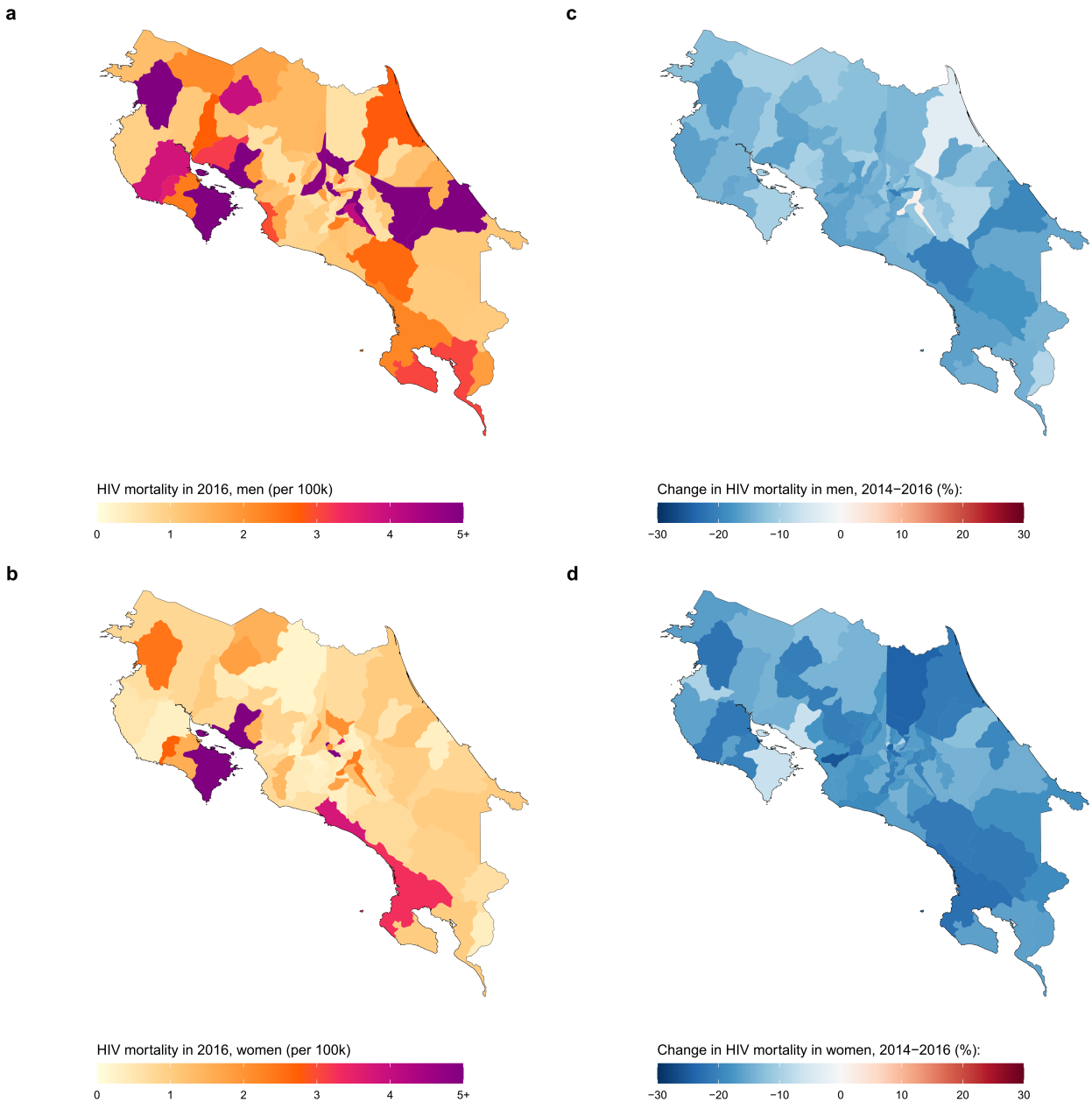

Figure 3: HIV mortality among men and women in Costa Rica by canton, 2016

HIV mortality per 100,000 by canton in Costa Rica in 2016 among men (a) and women (b). Relative change in HIV mortality between 2014 and 2016 among men (c) and women (d).

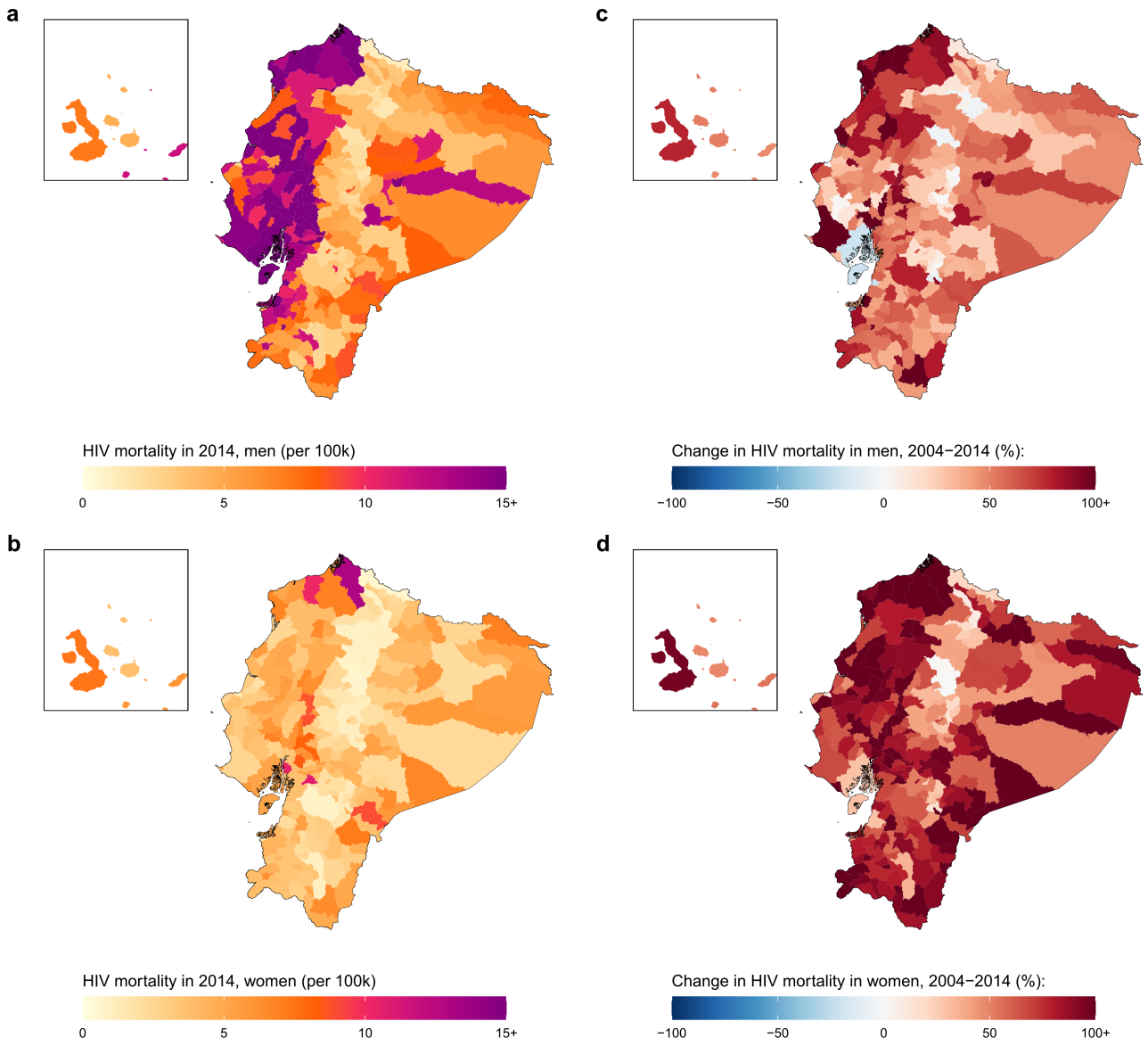

Figure 4: HIV mortality among men and women in Ecuador by canton, 2014

HIV mortality per 100,000 by canton in Ecuador in 2014 among men (a) and women (b). Relative change in HIV mortality between 2004 and 2014 among men (c) and women (d).

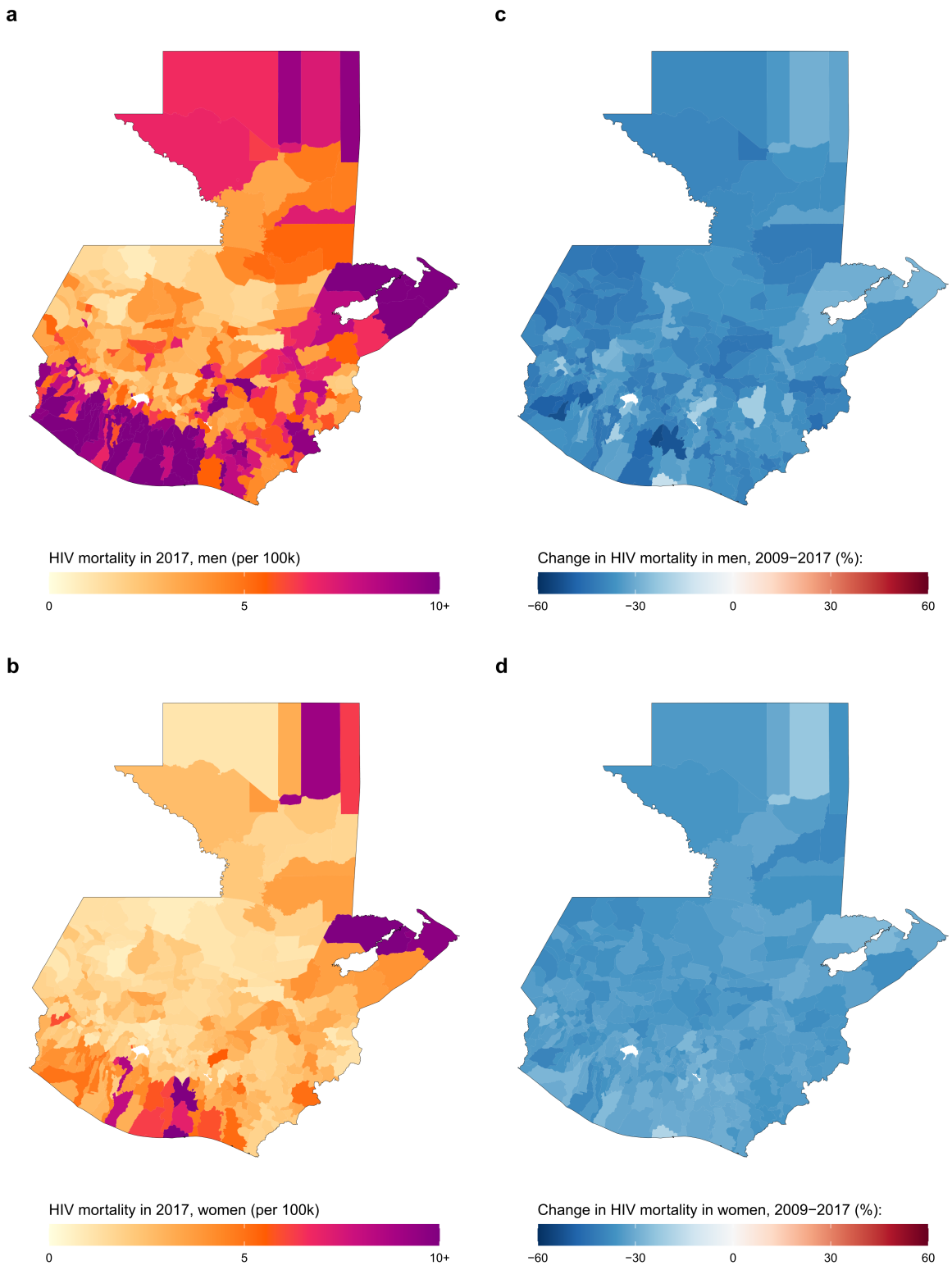

Figure 5: HIV mortality among men and women in Guatemala by municipality, 2017
HIV mortality per 100,000 by municipality in Guatemala in 2017 among men (a) and women (b). Relative change in HIV mortality between 2009 and 2017 among men (c) and women (d).

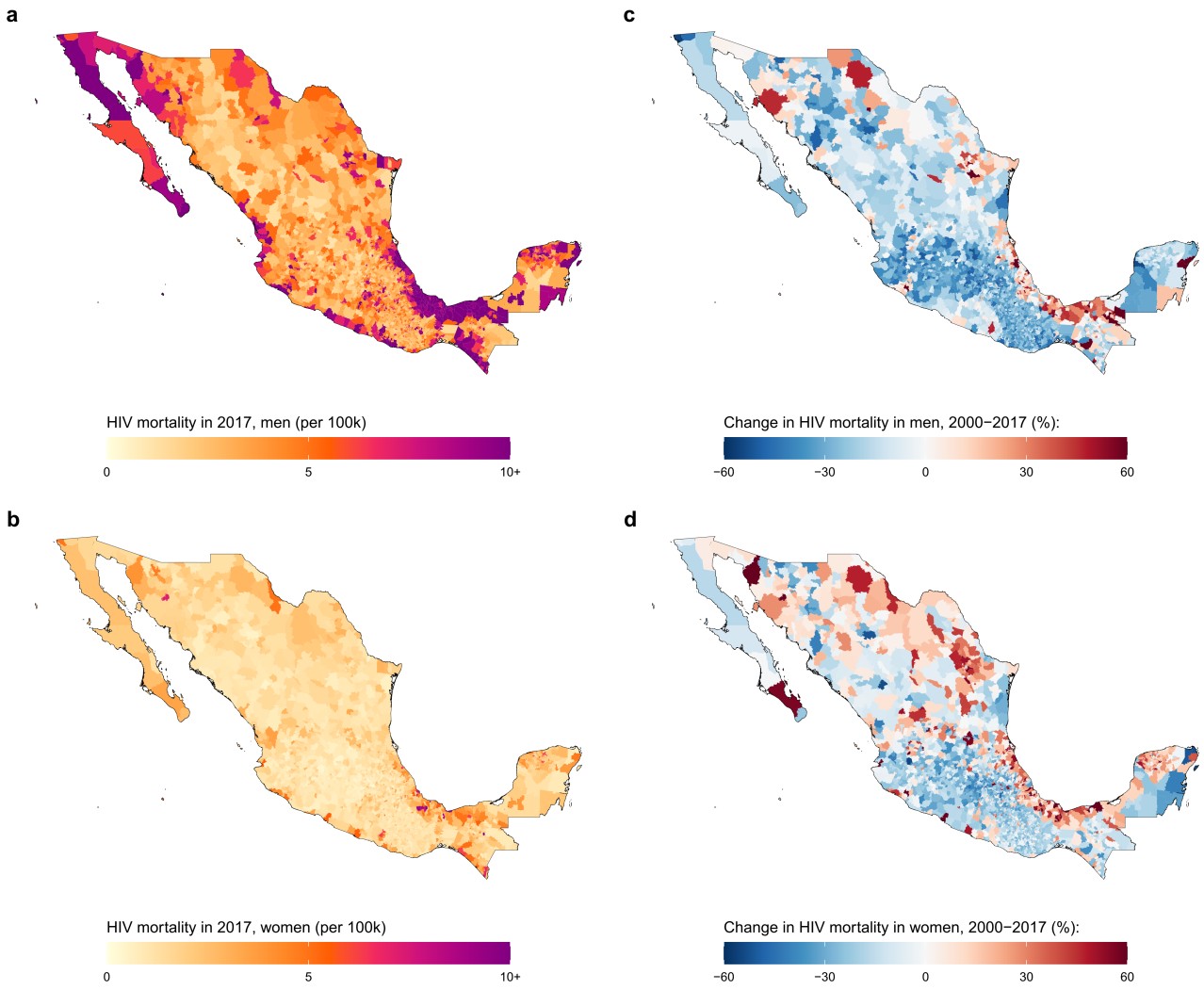

Figure 6: HIV mortality among men and women in Mexico by municipality, 2017

HIV mortality per 100,000 by municipality in Mexico in 2017 among men (a) and women (b). Relative change in HIV mortality between 2000 and 2017 among men (c) and women (d).

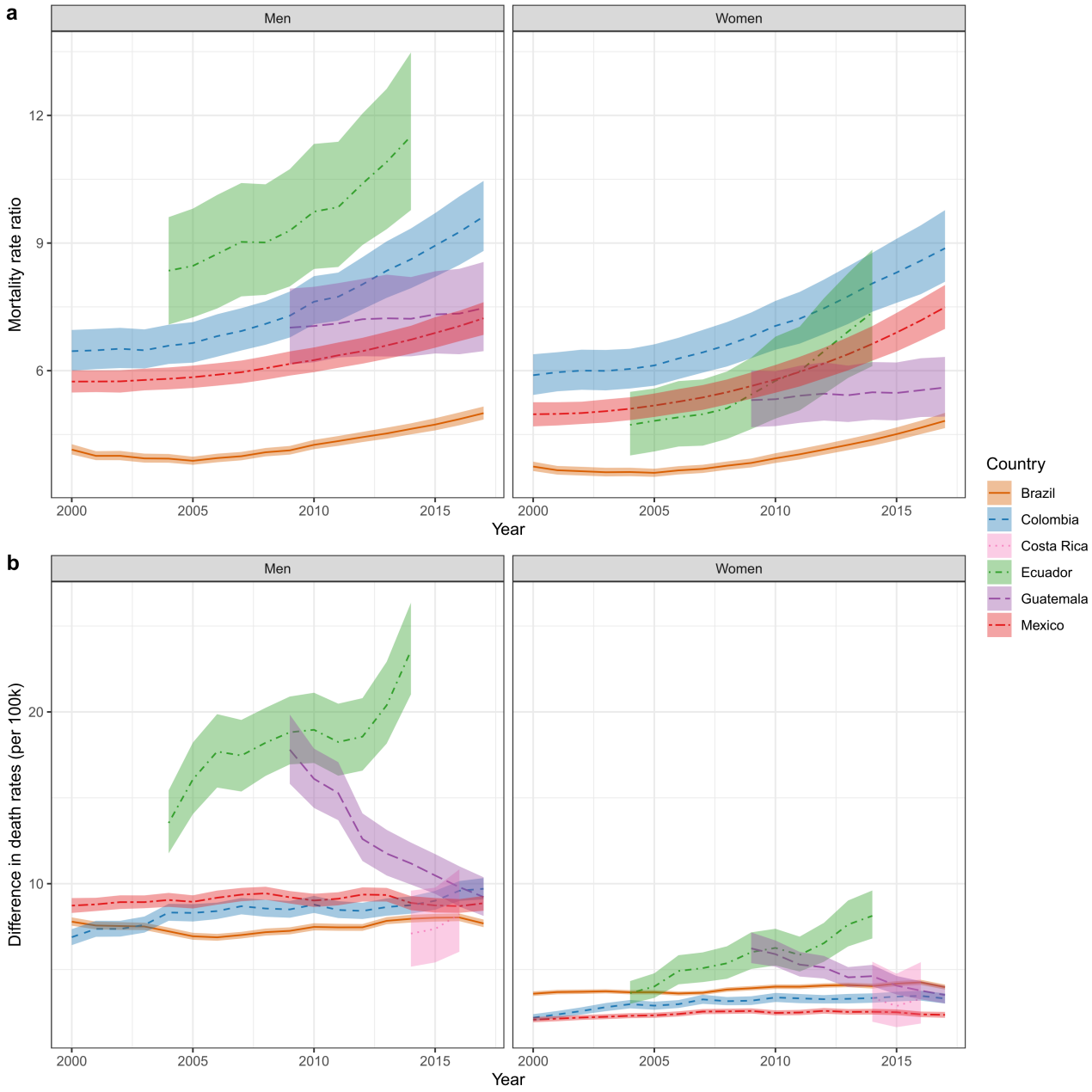

Figure 7: Relative and absolute inequality among municipalities in HIV mortality

Relative inequality, defined here as the ratio of estimated HIV mortality for municipalities in the 90th percentile versus 10th percentile, by year with 95% uncertainty intervals (a). Costa Rica is omitted from this panel because its estimated relative inequality was >50. Absolute inequality, defined here as the difference in HIV mortality rates for municipalities in the 90th versus 10th percentile, by year with 95% uncertainty intervals (b). Selected countries are differentiated by color and line type.

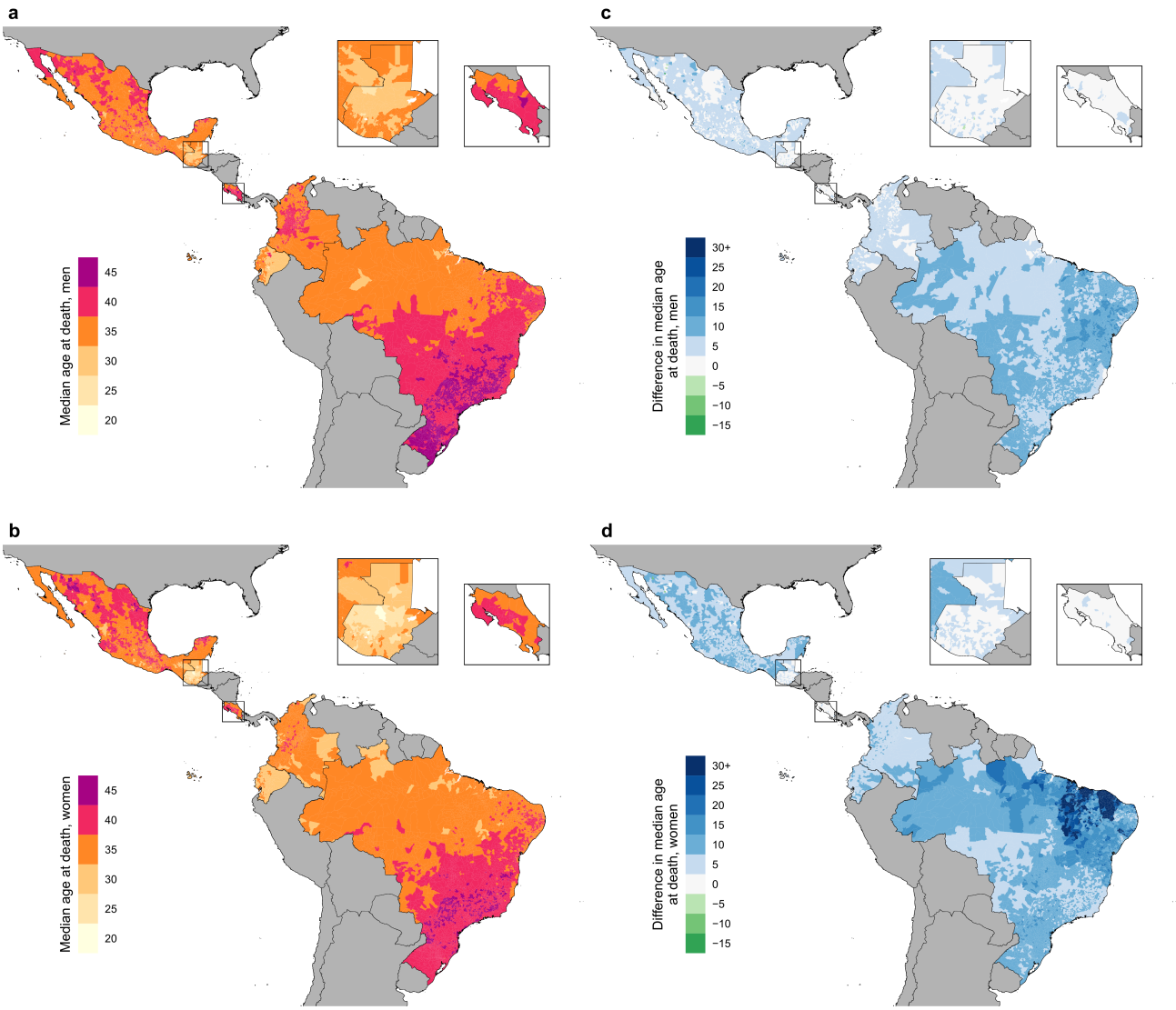

Figure 8: Estimated median age group among those who died from HIV, by municipality

Estimated median age of death among men (a) and women (b) who died from HIV in the last year of study in selected countries: 2017 in Brazil, Colombia, Guatemala, and Mexico, 2016 in Costa Rica, and 2014 in Ecuador. Estimated difference in median age of death among men (c) and women (d) who died from HIV from first year to last year of study in selected countries (2000–2017 in Brazil, Colombia, and Mexico, 2009–2017 in Guatemala, 2014–2016 in Costa Rica, and 2004–2014 in Ecuador).

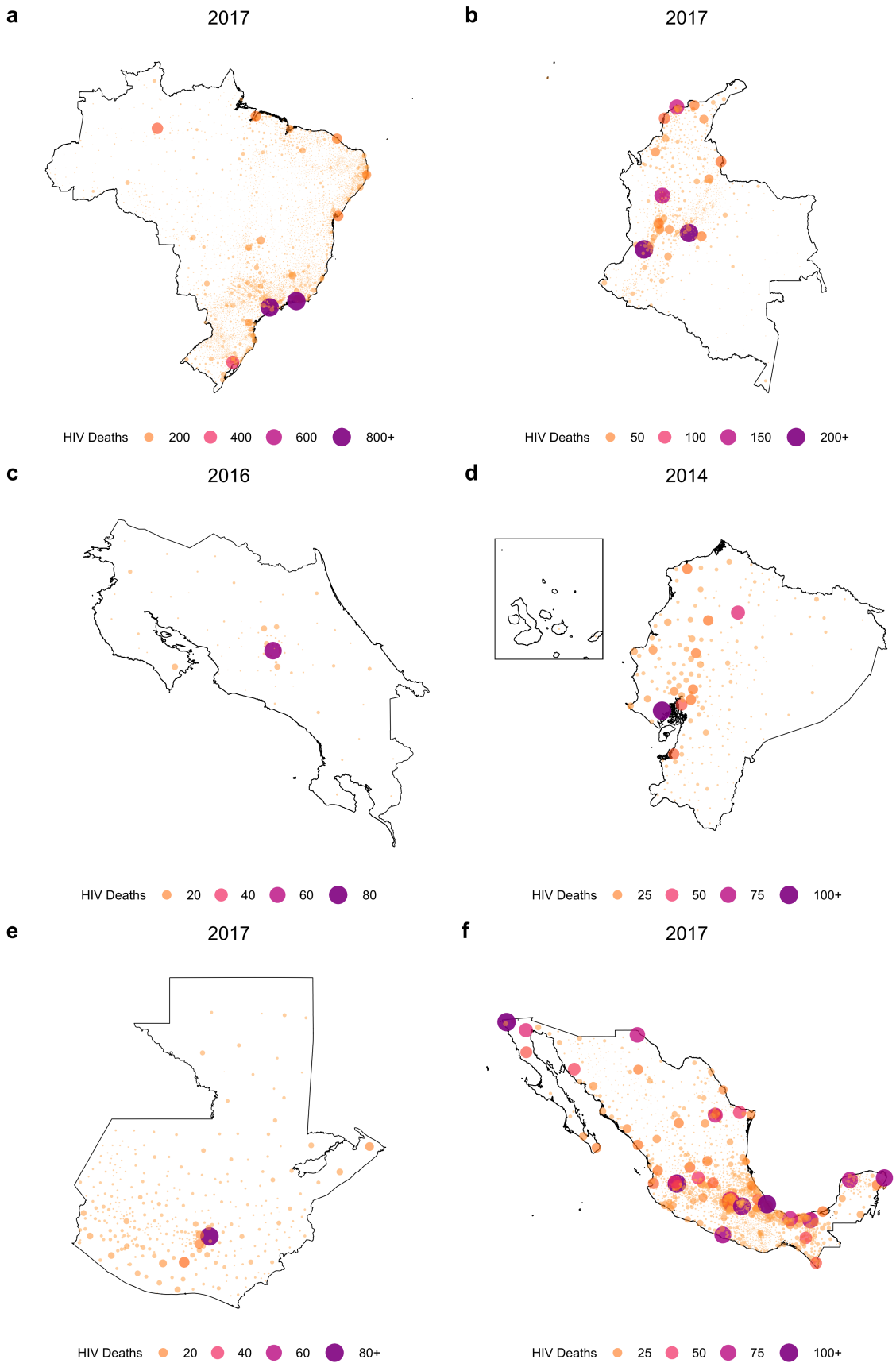
a
2017
HIV Deaths 200 400 600 800+
b
2017
HIV Deaths 50 100 150 200+
c
2016
HIV Deaths 20 40 60 80
d
2014
HIV Deaths 25 50 75 100+
e
2017
HIV Deaths 20 40 60 80+
f
2017
HIV Deaths 25 50 75 100+

Figure 9: Number of HIV deaths in latest year of study, by municipality

Estimated number of HIV deaths by municipallity in the latest year of study: 2017 in Brazil (a), 2017 in Colombia (b), 2016 in Costa Rica (c), 2014 in Ecuador (d), 2017 in Guatemala (e), 2017 in Mexico (f). Color and size are proportional to estimated HIV deaths.

References

1. Roth GA, Abate D, Abate KH, Abay SM, Abbafati C, Abbasi N, et al. Global, regional, and national age-sex-specific mortality for 282 causes of death in 195 countries and territories, 1980–2017: a systematic analysis for the Global Burden of Disease Study 2017. The Lancet. 2018;392:1736–88.

2. Frank TD, Carter A, Jahagirdar D, Biehl MH, Douwes-Schultz D, Larson SL, et al. Global, regional, and national incidence, prevalence, and mortality of HIV, 1980–2017, and forecasts to 2030, for 195 countries and territories: a systematic analysis for the Global Burden of Diseases, Injuries, and Risk Factors Study 2017. The Lancet HIV. 2019;6:e831–59.

3. Fast-Track - Ending the AIDS epidemic by 2030. https://www.unaids.org/en/resources/documents/2014/JC2686_WAD2014report. Accessed 23 Apr 2020.

4. Ravasi G, Grinsztejn B, Baruch R, Guanira JV, Luque R, Cáceres CF, et al. Towards a fair consideration of PrEP as part of combination HIV prevention in Latin America. J Int AIDS Soc. 2016;19 7Suppl 6. doi:10.7448/IAS.19.7.21113.

5. Joint United Nations Programme on HIV/AIDS. AIDSinfo. https://aidsinfo.unaids.org/. Accessed 23 Apr 2020.

6. Luz PM, Veloso VG, Grinsztejn B. The HIV epidemic in Latin America: accomplishments and challenges on treatment and prevention. Curr Opin HIV AIDS. 2019;14:366–73.

7. García JI, Sabidó M, Nikiforov M, Smith A, Hernández G, Ortiz R, et al. The UALE project: a cross-sectional approach for trends in HIV/STI prevalence among key populations attending STI clinics in Guatemala. BMJ Open. 2018;8:e022632.

8. Kerr LR, Kendall C, Guimarães M, Mota R, Veras MA, Dourado I, et al. HIV prevalence among men who have sex with men in Brazil: results of the 2nd national survey using respondent-driven sampling. Medicine. 2018;97:S9–15.

9. Colchero M, Romero M, Conde-Glez C, Sosa-Rubí S. Is the HIV Epidemic Stable among MSM in Mexico? HIV Prevalence and Risk Behavior Results from a Nationally Representative Survey among Men Who Have Sex with Men. PloS one. 2013;8:e72616.

10. Hebert JR, Hurley TG, Chiriboga DE, Barone J. A comparison of selected nutrient intakes derived from three diet assessment methods used in a low-fat maintenance trial. Public Health Nutrition. 1998;1:207–14.

11. Local Burden of Disease Child Growth Failure Collaborators. Mapping child growth failure across low- and middle-income countries. Nature. 2020;577:231–4.

12. Sgarbi RVE, Carbone A da SS, Paião DSG, Lemos EF, Simionatto S, Puga MAM, et al. A Cross-Sectional Survey of HIV Testing and Prevalence in Twelve Brazilian Correctional Facilities. PLoS ONE. 2015;10:e0139487.

13. Local Burden of Disease Educational Attainment Collaborators. Mapping disparities in education across low- and middle-income countries. Nature. 2020;577:235–8.

14. Tuboi SH, Schechter M, McGowan CC, Cesar C, Krolewiecki A, Cahn P, et al. Mortality during the first year of potent antiretroviral therapy in HIV-1-infected patients in 7 sites throughout Latin America and the Caribbean. J Acquir Immune Defic Syndr. 2009;51:615–23.

15. Ross J, Henry N, Dwyer-Lindgren L, Lobo A, Marinho de Souza MDF, Biehl M, et al. Progress toward eliminating TB and HIV deaths in Brazil, 2001-2015: A spatial assessment. BMC Medicine. 2018;16.

16. Alves ATJ, Nobre FF. The acquired immunodeficiency syndrome in the State of Rio de Janeiro, Brazil: a spatio-temporal analysis of cases reported in the period 2001-2010. Geospat Health. 2014;8:437–43.

17. de Holanda ER, Galvão MTG, Pedrosa NL, Paiva S de S, de Almeida RLF. Spatial analysis of infection by the human immunodeficiency virus among pregnant women. Rev Lat Am Enfermagem. 2015;23:441–9.

18. Pletcher. Model fittiing and hypothesis testing for age specific data. Journal of Evolutionary Biology. 2001;12:430–9.

19. Alexander M, Zagheni E, Barbieri M. A Flexible Bayesian Model for Estimating Subnational Mortality. Demography. 2016;54.

20. Ocaña-Riola R, Mayoral-Cortes JM. Spatio-temporal trends of mortality in small areas of Southern Spain. BMC public health. 2010;10:26.

21. Dwyer-Lindgren L, Squires E, Teeple S, Ikilezi G, Roberts D, Colombara D, et al. Small area estimation of under-5 mortality in Bangladesh, Cameroon, Chad, Mozambique, Uganda, and Zambia using spatially misaligned data. Population Health Metrics. 2018;16.

22. Murray CJL, Ortblad KF, Guinovart C, Lim SS, Wolock TM, Roberts DA, et al. Global, regional, and national incidence and mortality for HIV, tuberculosis, and malaria during 1990–2013: a systematic analysis for the Global Burden of Disease Study 2013. Lancet. 2014;384:1005–70.

23. Carvalho CN, Dourado I, Bierrenbach AL. Underreporting of the tuberculosis and AIDS comorbidity: an application of the linkage method. Rev Saude Publica. 2011;45:548–55.

24. Birnbaum J, Murray C, Lozano R. Exposing misclassified HIV/AIDS deaths in South Africa. Bulletin of the World Health Organisation. 2011;89:278–85.

25. Lima EEC, Queiroz BL, Zeman K. Completeness of birth registration in Brazil: an overview of methods and data sources. Genus. 2018;74. doi:10.1186/s41118-018-0035-9.

26. Mikkelsen L, Phillips DE, AbouZahr C, Setel PW, de Savigny D, Lozano R, et al. A global assessment of civil registration and vital statistics systems: monitoring data quality and progress. The Lancet. 2015;386:1395–406.

27. BHAT P. Completeness of India's Sample Registration System: An assessment using the general growth balance method. Population studies. 2002;56:119–34.

28. Murray C, Rajaratnam J, Marcus J, Laakso T, Lopez A. What Can We Conclude from Death Registration? Improved Methods for Evaluating Completeness. PLoS medicine. 2010;7:e1000262.

29. Adair T, Lopez AD. Estimating the completeness of death registration: An empirical method. PLoS One. 2018;13. doi:10.1371/journal.pone.0197047.

30. Schmertmann CP, Gonzaga MR. Bayesian Estimation of Age-Specific Mortality and Life Expectancy for Small Areas With Defective Vital Records. Demography. 2018;55:1363–88.

31. Stevens GA, Alkema L, Black RE, Boerma JT, Collins GS, Ezzati M, et al. Guidelines for Accurate and Transparent Health Estimates Reporting: the GATHER statement. The Lancet. 2016;388:e19–23.

32. World Health Organization. ICD-10: International statistical classification of diseases and related health problems. 1992.

33. Naghavi M, Makela S, Foreman K, O'Brien J, Pourmalek F, Lozano R. Algorithms for enhancing public health utility of national causes-of-death data. Popul Health Metr. 2010;8:9.

34. GADM. https://gadm.org/. Accessed 17 Mar 2020.

35. Global Administrative Unit Layers (GAUL). http://www.fao.org/geonetwork/srv/en/metadata.show?id=12691. Accessed 27 May 2020.

36. Humanitarian Data Exchange. https://data.humdata.org/. Accessed 27 May 2020.

37. ArcMap. https://desktop.arcgis.com/en/arcmap/. Accessed 14 Jun 2020.

38. WorldPop. https://www.worldpop.org/project/categories?id=3. Accessed 17 Mar 2020.

39. Earth Observation Group - Defense Meteorological Satellite Progam, Boulder | ngdc.noaa.gov. https://www.ngdc.noaa.gov/eog/dmsp/downloadV4composites.html. Accessed 17 Mar 2020.

40. Global Human Settlement - Data overview - European Commission. https://ghsl.jrc.ec.europa.eu/data.php. Accessed 17 Mar 2020.

41. Weiss D, Nelson A, Gibson H, Temperley W, Peedell S, Lieber A, et al. A global map of travel time to cities to assess inequalities in accessibility in 2015. Nature. 2018;553.

42. Burstein R, Henry N, Collison M, Marczak L, Sligar A, Watson S, et al. Mapping 123 million neonatal, infant and child deaths between 2000 and 2017. Nature. 2019;574:353–358.

43. Målqvist M, Eriksson L, Nga N, Fagerland L, Hoa D, Ewald U, et al. Unreported births and deaths, a severe obstacle for improved neonatal survival in low-income countries; a population based study. BMC international health and human rights. 2008;8:4.

44. Dwyer-Lindgren L, Bertozzi-Villa A, Stubbs RW, Morozoff C, Kutz MJ, Huynh C, et al. US County-Level Trends in Mortality Rates for Major Causes of Death, 1980-2014. JAMA. 2016;316:2385–401.

45. Leroux BG, Lei X, Breslow N. Estimation of Disease Rates in Small Areas: A new Mixed Model for Spatial Dependence. In: Halloran ME, Berry D, editors. Statistical Models in Epidemiology, the Environment, and Clinical Trials. New York, NY: Springer; 2000. p. 179–91.

46. Knorr-Held L. Bayesian modelling of inseparable space-time variation in disease risk. Stat Med. 2000;19:2555–67.

47. Kristensen K, Nielsen A, Berg CW, Skaug H, Bell BM. TMB: Automatic Differentiation and Laplace Approximation. Journal of Statistical Software. 2016;70:1–21.

48. R Core Team. R: a language and environment for statistical computing. Vienna, Austria: Foundation for Statistical Computing; 2015.

49. Alonso Gonzalez M, Martin L, Munoz S, Jacobson JO. Patterns, trends and sex differences in HIV/AIDS reported mortality in Latin American countries: 1996-2007. BMC Public Health. 2011;11:605.

50. Bozon M, Gayet C, Barrientos J. A Life Course Approach to Patterns and Trends in Modern Latin American Sexual Behavior. Journal of acquired immune deficiency syndromes (1999). 2009;51 Suppl 1:S4–12.

51. Miller WM, Buckingham L, Sánchez-Domínguez MS, Morales-Miranda S, Paz-Bailey G. Systematic review of HIV prevalence studies among key populations in Latin America and the Caribbean. Salud Publica Mex. 2013;55 Suppl 1:S65-78.

52. Dolan K, Kite B, Black E, Aceijas C, Stimson G. HIV in prison I low-income and middle-income countries. The Lancet infectious diseases. 2007;7:32–41.

53. Prellwitz IM, Alves BM, Ikeda MLR, Kuhleis D, Picon PD, Jarczewski CA, et al. HIV behind Bars: Human Immunodeficiency Virus Cluster Analysis and Drug Resistance in a Reference Correctional Unit from Southern Brazil. PLoS One. 2013;8. doi:10.1371/journal.pone.0069033.

54. Crabtree-Ramírez B, Belaunzarán-Zamudio PF, Cortes CP, Morales M, Sued O, Sierra-Madero J, et al. The HIV epidemic in Latin America: a time to reflect on the history of success and the challenges ahead. J Int AIDS Soc. 2020;23. doi:10.1002/jia2.25468.

55. Carriquiry G, Fink V, Koethe JR, Giganti MJ, Jayathilake K, Blevins M, et al. Mortality and loss to follow-up among HIV-infected persons on long-term antiretroviral therapy in Latin America and the Caribbean. J Int AIDS Soc. 2015;18:20016.

56. Caro-Vega Y, Belaunzarán-Zamudio PF, Crabtree-Ramírez B, Shepherd BE, Mejia F, Giganti MJ, et al. Trends in proportion of older HIV-infected people in care in Latin America and the Caribbean: A growing challenge. Epidemiology and infection. 2018;146:1308.

57. Mpondo BCT. HIV Infection in the Elderly: Arising Challenges. J Aging Res. 2016;2016. doi:10.1155/2016/2404857.

58. Nash D, Katyal M, Brinkhof MWG, Keiser O, May M, Hughes R, et al. Long-term immunologic response to antiretroviral therapy in low-income countries: Collaborative analysis of prospective studies. AIDS. 2008;22:2291–302.

59. Hoagland B, Moreira RI, De Boni RB, Kallas EG, Madruga JV, Vasconcelos R, et al. High pre-exposure prophylaxis uptake and early adherence among men who have sex with men and transgender women at risk for HIV Infection: the PrEP Brasil demonstration project. J Int AIDS Soc. 2017;20:21472.

60. Gomez GB, Borquez A, Caceres CF, Segura ER, Grant RM, Garnett GP, et al. The potential impact of pre-exposure prophylaxis for HIV prevention among men who have sex with men and transwomen in Lima, Peru: a mathematical modelling study. PLoS Med. 2012;9:e1001323.

61. UNAIDS. Global AIDS update 2018: Miles to go. 2018. https://www.unaids.org/sites/default/files/media_asset/miles-to-go_en.pdf. Accessed 4 Jun 2019.

62. Anderson S-J, Cherutich P, Kilonzo N, Cremin I, Fecht D, Kimanga D, et al. Maximising the effect of combination HIV prevention through prioritisation of the people and places in greatest need: a modelling study. The Lancet. 2014;384:249–56.

63. Gerberry DJ, Wagner BG, Garcia-Lerma JG, Heneine W, Blower S. Using geospatial modelling to optimize the rollout of antiretroviral-based pre-exposure HIV interventions in Sub-Saharan Africa. Nature Communications. 2014;5:ncomms6454.

64. Stevens FR, Gaughan AE, Linard C, Tatem AJ. Disaggregating Census Data for Population Mapping Using Random Forests with Remotely-Sensed and Ancillary Data. PLOS ONE. 2015;10:e0107042. doi:10.1371/journal.pone.0107042.

Supplementary Appendix: Mapping HIV mortality in six Latin American countries using incomplete vital registration systems

Table of Contents

Compliance with the Guidelines for Accurate and Transparent Health Estimates Reporting (GATHER)

Item #	Checklist item	Description of Compliance
Objectives and funding		
1	Define the indicator(s), populations (including age, sex, and geographical entities), and time period(s) for which estimates were made.	Manuscript: Background, Methods
2	List the funding sources for the work.	Manuscript: Declarations (Funding)
Data Inputs		
For all data inputs from multiple sources that are synthesised as part of the study:		
3	Describe how the data were identified and how the data were accessed.	Manuscript: Methods
4	Specify the inclusion and exclusion criteria. Identify all ad-hoc exclusions.	Manuscript: Methods
5	Provide information on all included data sources and their main characteristics. For each data source used, report reference information or contact name/institution, population represented, data collection method, year(s) of data collection, sex and age range, diagnostic criteria or measurement method, and sample size, as relevant.	Supplementary Tables 1 and 2
6	Identify and describe any categories of input data that have potentially important biases (e.g., based on characteristics listed in item 5).	Manuscript: Discussion (Limitations)
For data inputs that contribute to the analysis but were not synthesised as part of the study:		
7	Describe and give sources for any other data inputs.	
For all data inputs:		
8	Provide all data inputs in a file format from which data can be efficiently extracted (e.g., a spreadsheet rather than a PDF), including all relevant meta-data listed in item 5. For any data inputs that cannot be shared because of ethical or legal reasons, such as third-party ownership, provide a contact name or the name of the institution that retains the right to the data.	Available through GHDx link (upon publication)
Data analysis		
9	Provide a conceptual overview of the data analysis method. A diagram may be helpful.	Manuscript: Methods
10	Provide a detailed description of all steps of the analysis, including mathematical formulae. This description should cover, as relevant, data cleaning, data pre-processing, data adjustments and weighting of data sources, and mathematical or statistical model(s).	Manuscript: Methods
11	Describe how candidate models were evaluated and how the final model(s) were selected.	Manuscript: Methods

12	Provide the results of an evaluation of model performance, if done, as well as the results of any relevant sensitivity analysis.	
13	Describe methods for calculating uncertainty of the estimates. State which sources of uncertainty were, and were not, accounted for in the uncertainty analysis.	Manuscript: Methods
14	State how analytic or statistical source code used to generate estimates can be accessed.	Available through GHDx link (upon publication)
Results and Discussion		
15	Provide published estimates in a file format from which data can be efficiently extracted.	Available through GHDx link (upon publication)
16	Report a quantitative measure of the uncertainty of the estimates (e.g., uncertainty intervals).	Manuscript: Results
17	Interpret results in light of existing evidence. If updating a previous set of estimates, describe the reasons for changes in estimates.	Manuscript: Discussion
18	Discuss limitations of the estimates. Include a discussion of any modelling assumptions or data limitations that affect interpretation of the estimates.	Manuscript: Discussion

Supplemental Figures

Figure S1: Model alignment with GBD, Brazil

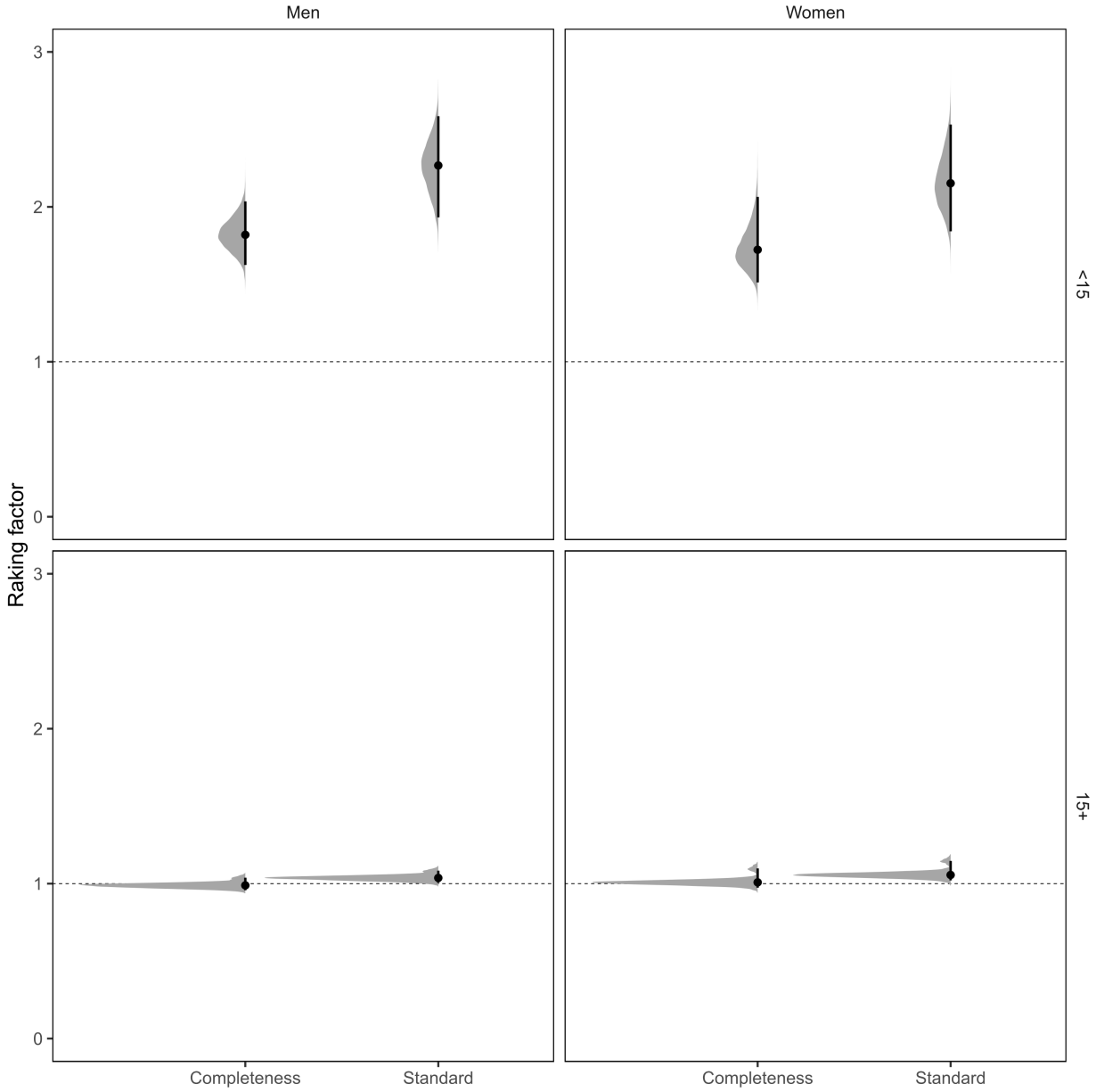

Figure S1: Model alignment with GBD, Brazil. Comparison of the annual ratio of national HIV mortality from GBD and 1,000 draws of annual national HIV mortality in children under-15 (<15) and adults (15+) by sex across the entire range of study (2000 to 2017). The model used in the analysis that includes prior completeness π_{k,t,a^*} ('Completeness') is shown compared to a model without any prior information on completeness ('Standard'). Each point represents the median of the draws of the raking factor, and the bar represents 2.5th and 97.5th quantile of the draws.

Figure S2: Model alignment with GBD, Colombia

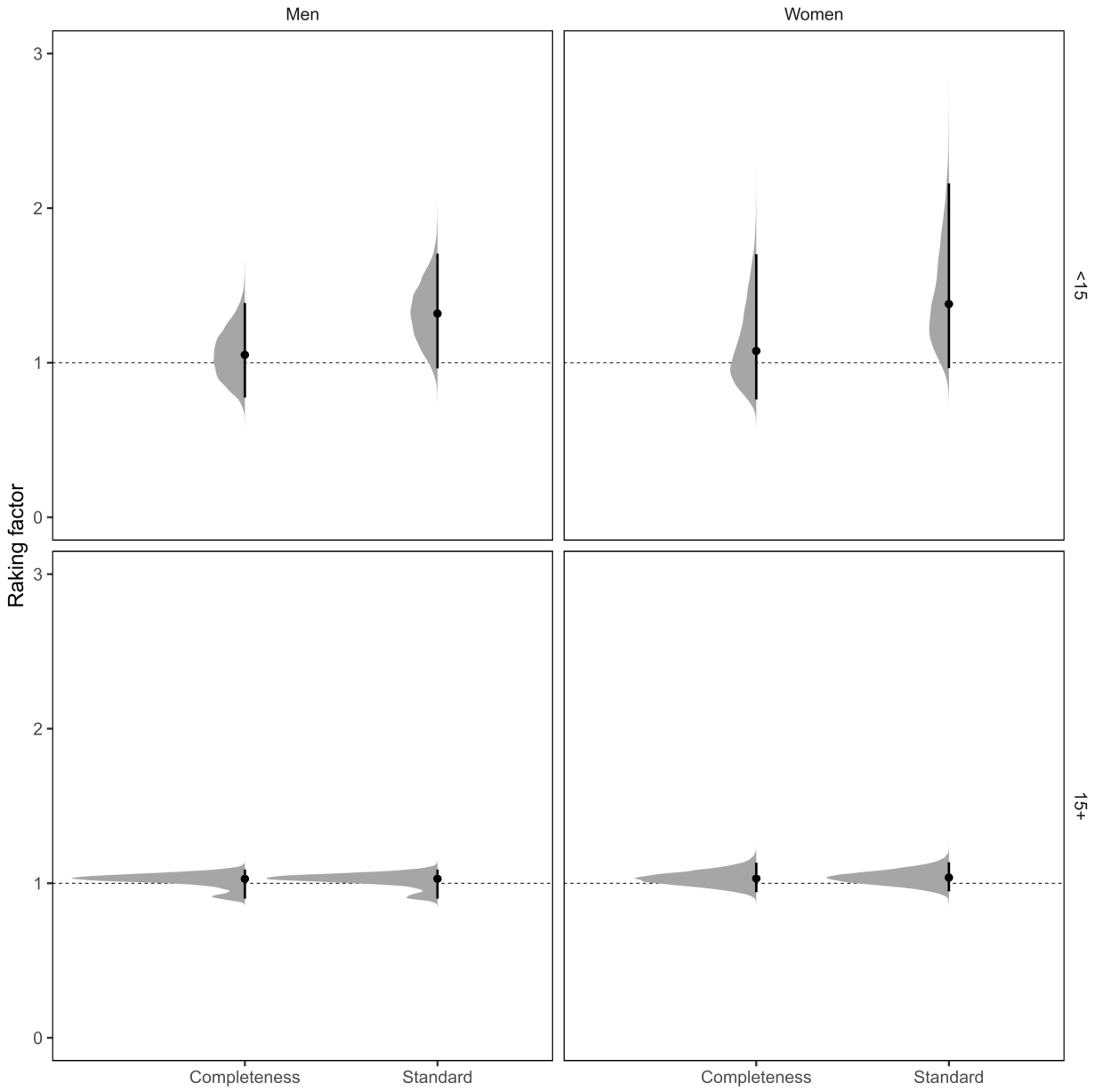

Figure S2: Model alignment with GBD, Colombia. Comparison of the annual ratio of national HIV mortality from GBD and 1,000 draws of annual national HIV mortality in children under-15 (<15) and adults (15+) by sex across the entire range of study (2000 to 2017). The model used in the analysis that includes prior completeness π_{k,t,a^*} ('Completeness') is shown compared to a model without any prior information on completeness ('Standard'). Each point represents the median of the draws of the raking factor, and the bar represents 2.5th and 97.5th quantile of the draws.

Figure S3: Model alignment with GBD, Costa Rica

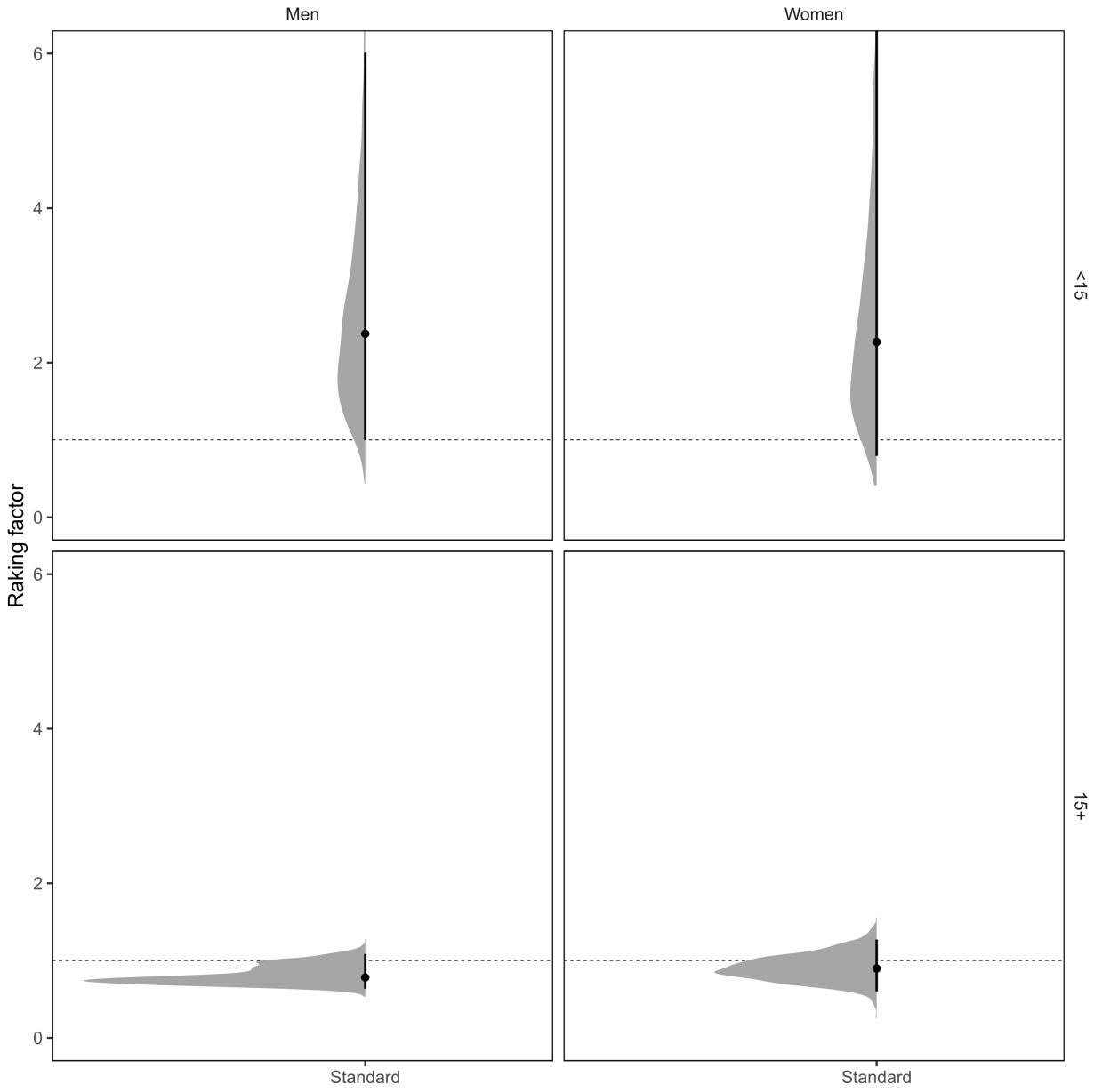

Figure S3: Model alignment with GBD, Costa Rica. Comparison of the annual ratio of national HIV mortality from GBD and 1,000 draws of annual national HIV mortality in children under-15 (<15) and adults (15+) by sex across the entire range of the study (2014 to 2016). We do not model prior completeness for Costa Rica, and we show the final model without any prior information on completeness ('Standard'). Each point represents the median of the draws of the raking factor, and the bar represents 2.5th and 97.5th quantile of the draws.

Figure S4: Model alignment with GBD, Ecuador

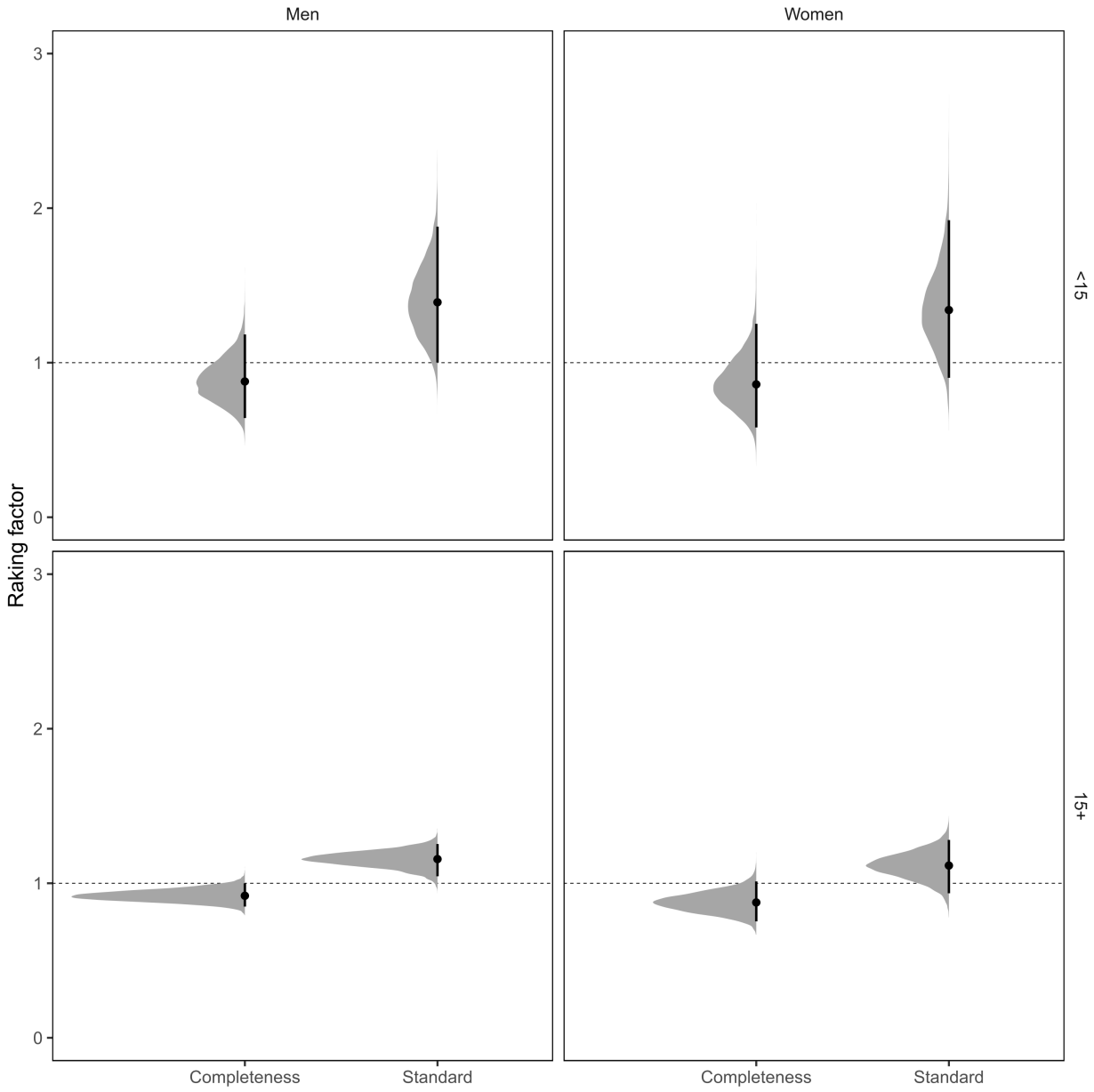

Figure S4: Model alignment with GBD, Ecuador. Comparison of the annual ratio of national HIV mortality from GBD and 1,000 draws of annual national HIV mortality in children under-15 (<15) and adults (15+) by sex across the entire range of study (2004 to 2014). The model used in the analysis that includes prior completeness π_{k,t,a^*} ('Completeness') is shown compared to a model without any prior information on completeness ('Standard'). Each point represents the median of the draws of the raking factor, and the bar represents 2.5th and 97.5th quantile of the draws.

Figure S5: Model alignment with GBD, Guatemala

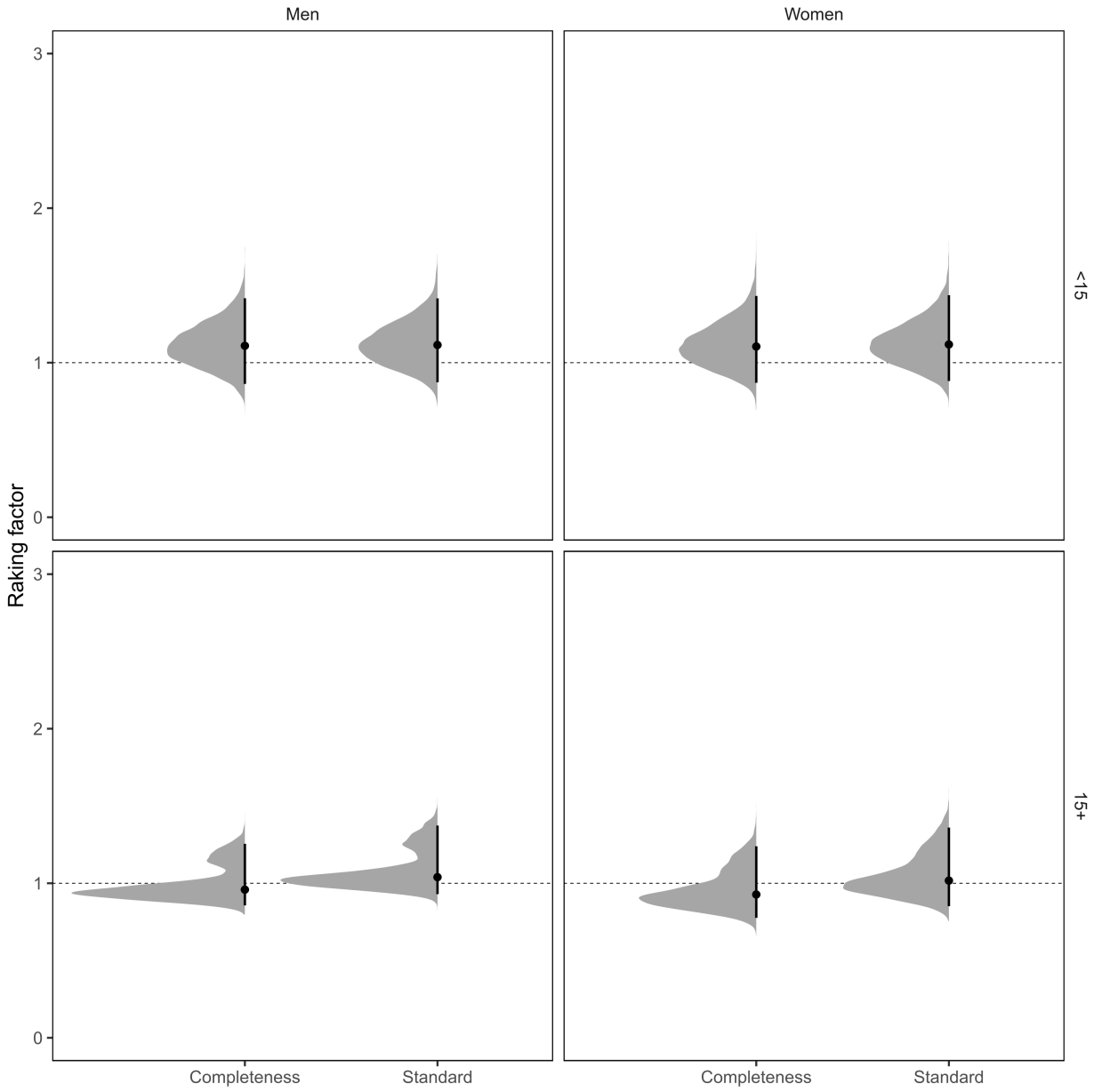

Figure S5: Model alignment with GBD, Guatemala. Comparison of the annual ratio of national HIV mortality from GBD and 1,000 draws of annual national HIV mortality in children under-15 (<15) and adults (15+) by sex across the entire range of study (2009 to 2017). The model used in the analysis that includes prior completeness π_{k,t,a^*} ('Completeness') is shown compared to a model without any prior information on completeness ('Standard'). Each point represents the median of the draws of the raking factor, and the bar represents 2.5th and 97.5th quantile of the draws.

Figure S6: Model alignment with GBD, Mexico

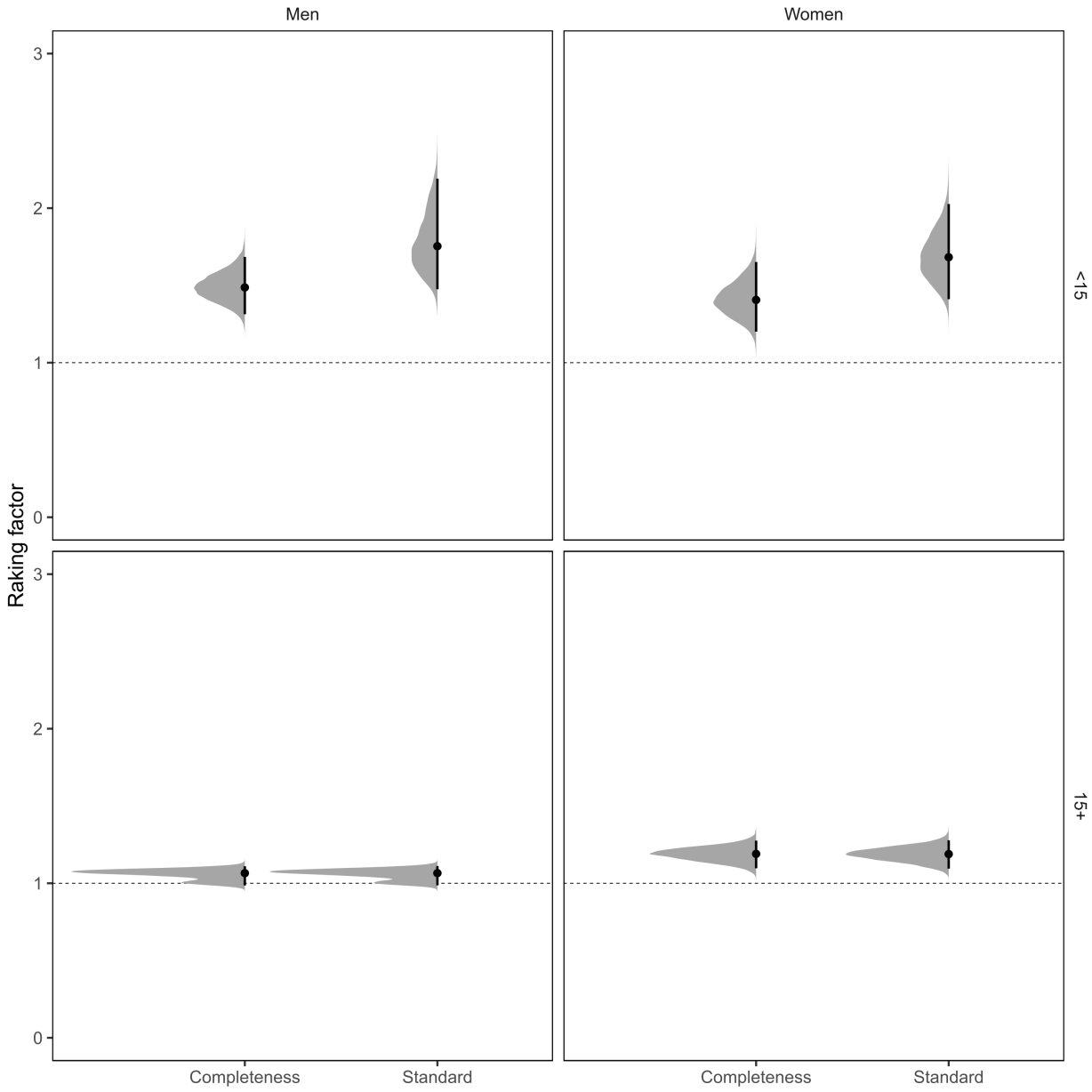

Figure S6: Model alignment with GBD, Mexico. Comparison of the annual ratio of national HIV mortality from GBD and 1,000 draws of annual national HIV mortality in children under-15 (<15) and adults (15+) by sex across the entire range of study (2000 to 2017). The model used in the analysis that includes prior completeness π_{k,t,a^*} ('Completeness') is shown compared to a model without any prior information on completeness ('Standard'). Each point represents the median of the draws of the raking factor, and the bar represents 2.5th and 97.5th quantile of the draws.

Figure S7: Uncertainty in estimated HIV mortality in Brazil, 2017

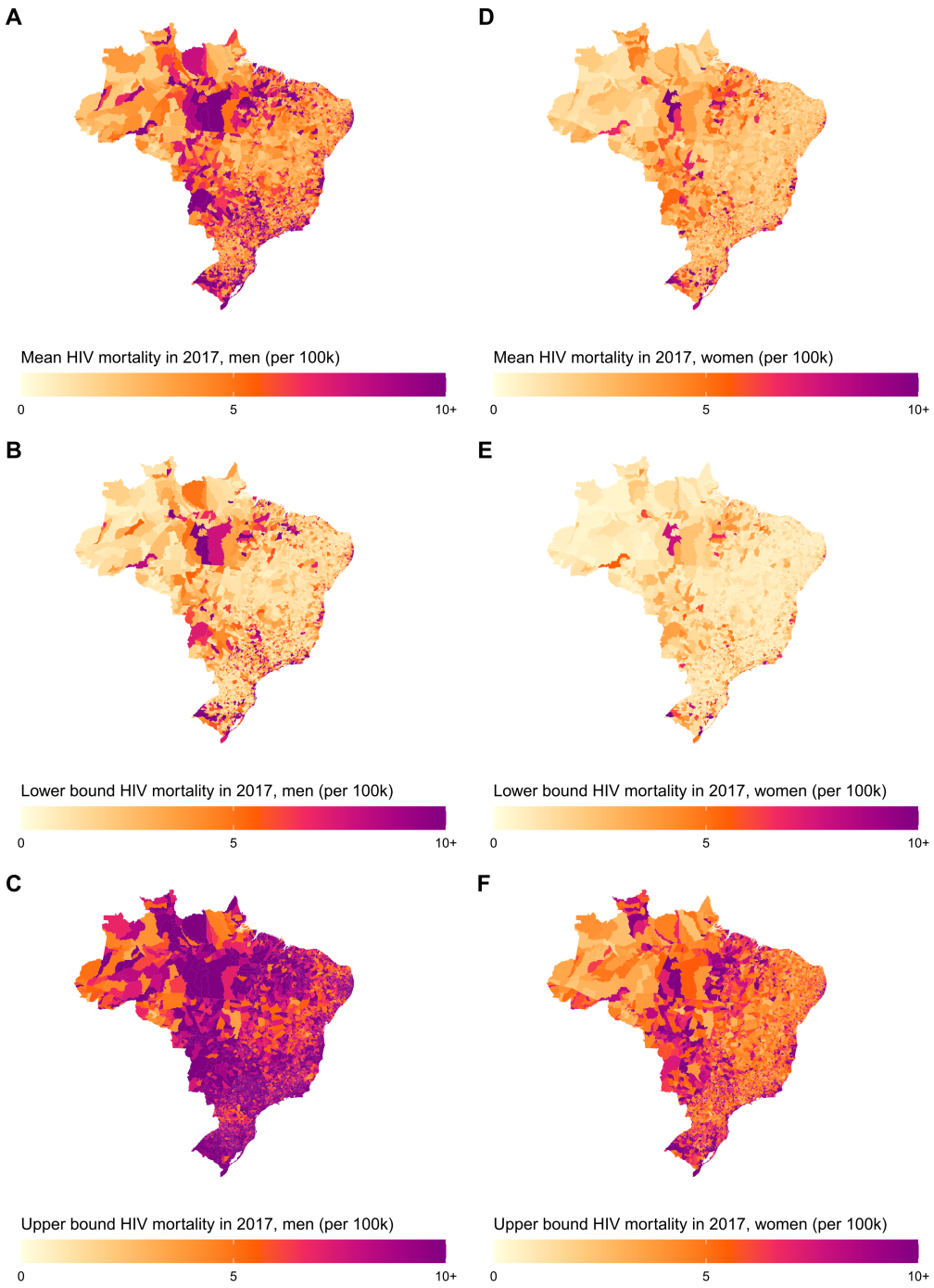

Figure S7: Uncertainty in estimated HIV mortality in Brazil, 2017. Estimated HIV mortality at the municipality level in 2017 in Brazil among men (**a-c**) and women (**d-f**). Mean estimates and lower and upper bounds of the 95% uncertainty intervals are shown in the top, middle, and bottom column, respectively.

Figure S8: Uncertainty in estimated HIV mortality in Colombia, 2017

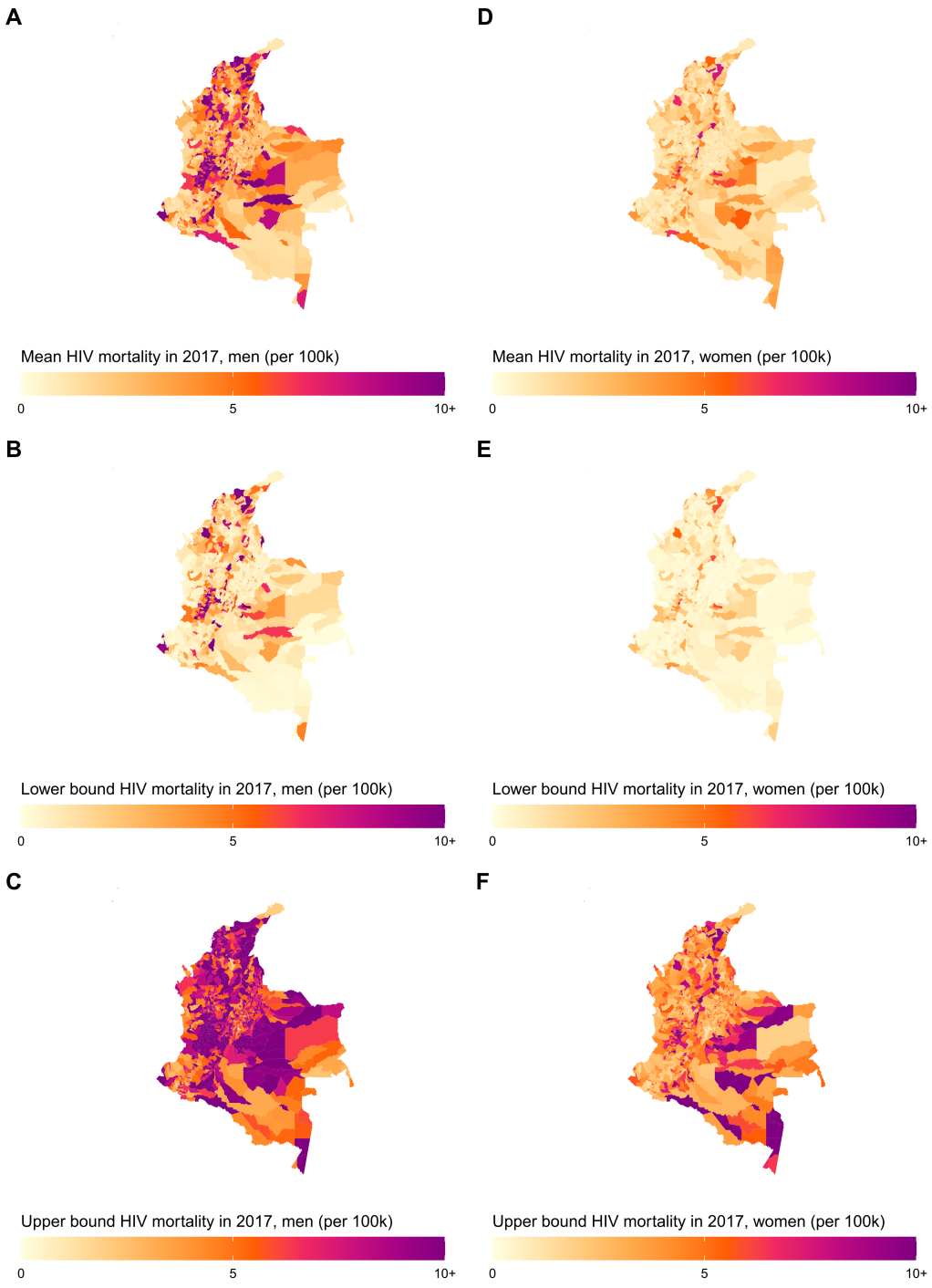

Figure S8: Uncertainty in estimated HIV mortality in Colombia, 2017. Estimated HIV mortality at the municipality level in 2017 in Colombia among men (**a-c**) and women (**d-f**). Mean estimates and lower and upper bounds of the 95% uncertainty intervals are shown in the top, middle, and bottom column, respectively.

Figure S9: Uncertainty in estimated HIV mortality in Costa Rica, 2016

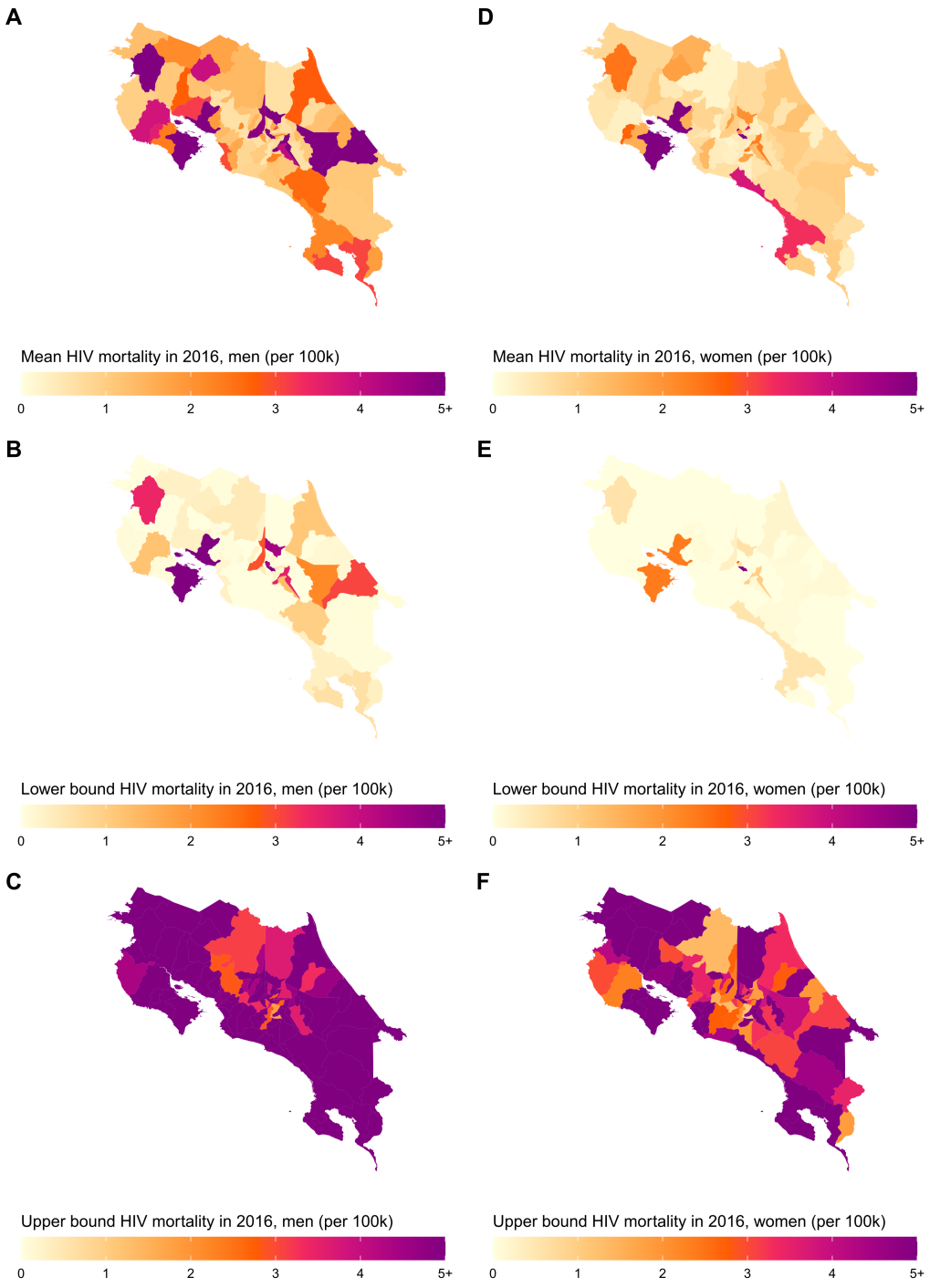

Figure S9: Uncertainty in estimated HIV mortality in Costa Rica, 2016. Estimated HIV mortality at the canton level in 2016 in Costa Rica among men (**a-c**) and women (**d-f**). Mean estimates and lower and upper bounds of the 95% uncertainty intervals are shown in the top, middle, and bottom column, respectively.

Figure S10: Uncertainty in estimated HIV mortality in Ecuador, 2014

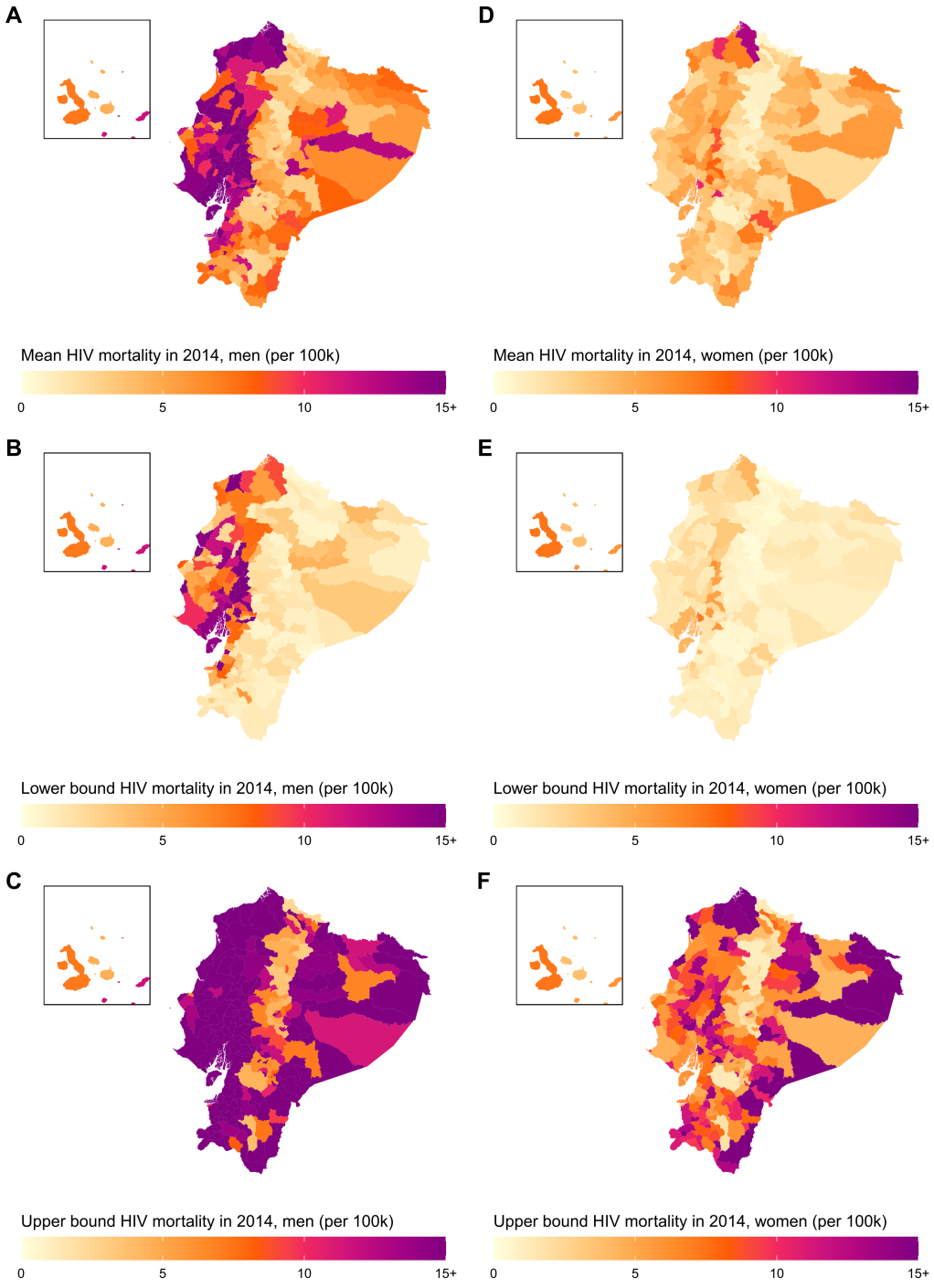

Figure S10: Uncertainty in estimated HIV mortality in Ecuador, 2014. Estimated HIV mortality at the canton level in 2014 in Ecuador among men (**a-c**) and women (**d-f**). Mean estimates and lower and upper bounds of the 95% uncertainty intervals are shown in the top, middle, and bottom column, respectively.

Figure S11: Uncertainty in estimated HIV mortality in Guatemala, 2017

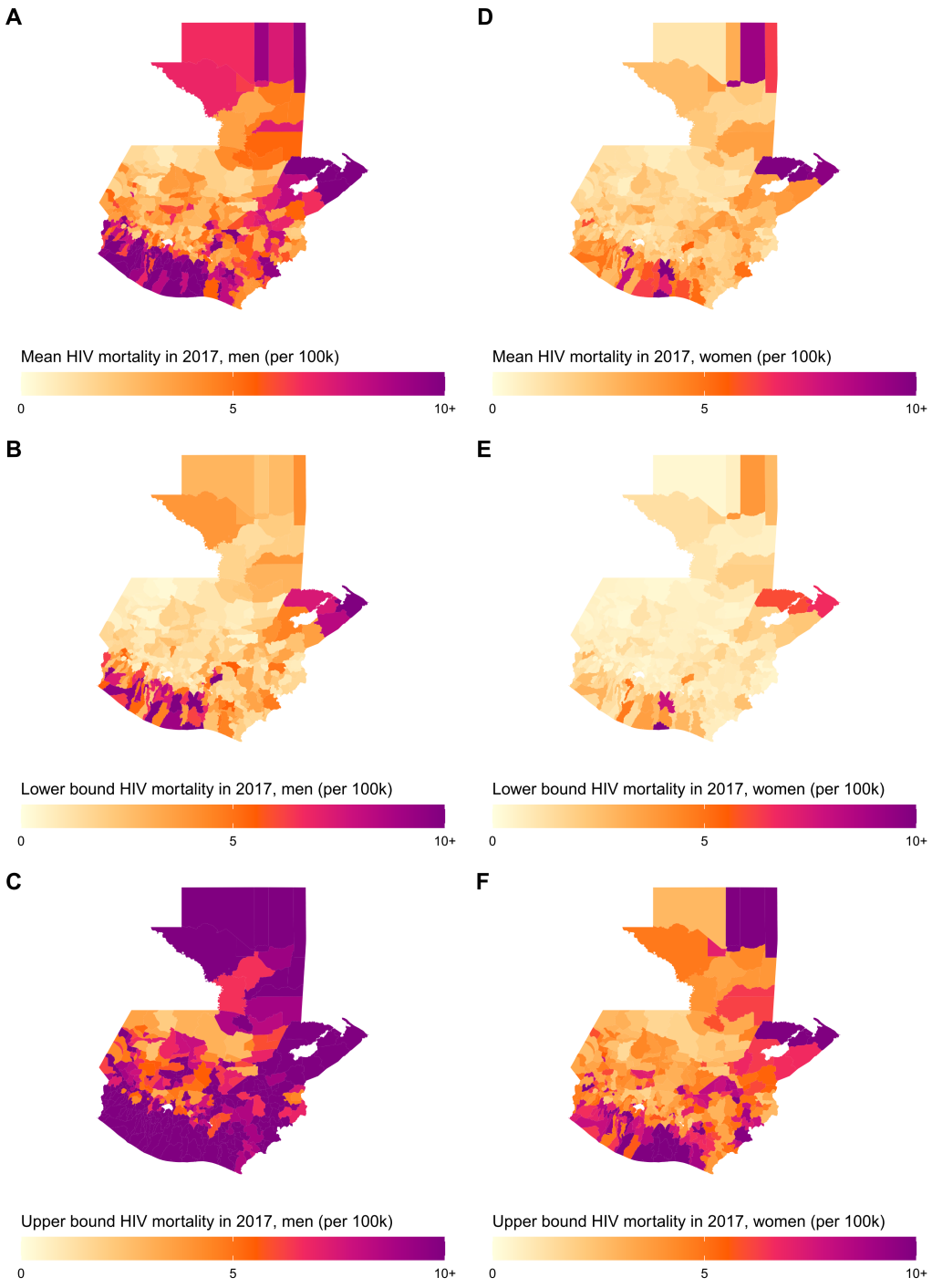

Figure S11: Uncertainty in estimated HIV mortality in Guatemala, 2017. Estimated HIV mortality at the municipality level in 2017 in Guatemala among men (**a-c**) and women (**d-f**). Mean estimates and lower and upper bounds of the 95% uncertainty intervals are shown in the top, middle, and bottom column, respectively.

Figure S12: Uncertainty in estimated HIV mortality in Mexico, 2017

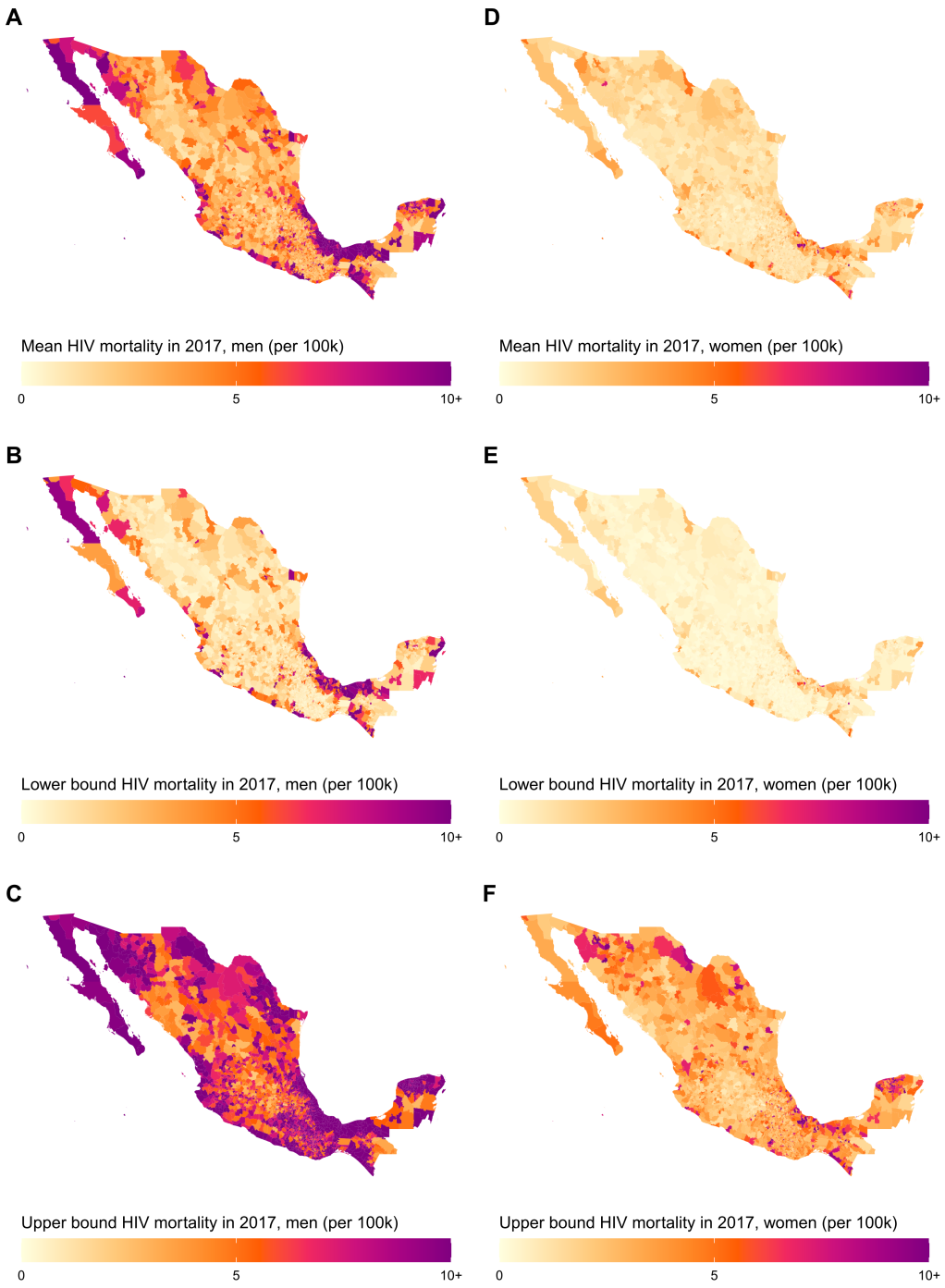

Figure S12: Uncertainty in estimated HIV mortality in Mexico, 2017. Estimated HIV mortality at the municipality level in 2017 in Mexico among men (**a-c**) and women (**d-f**). Mean estimates and lower and upper bounds of the 95% uncertainty intervals are shown in the top, middle, and bottom column, respectively.

Figure S13: Estimated HIV mortality in Brazil by age group, 2017

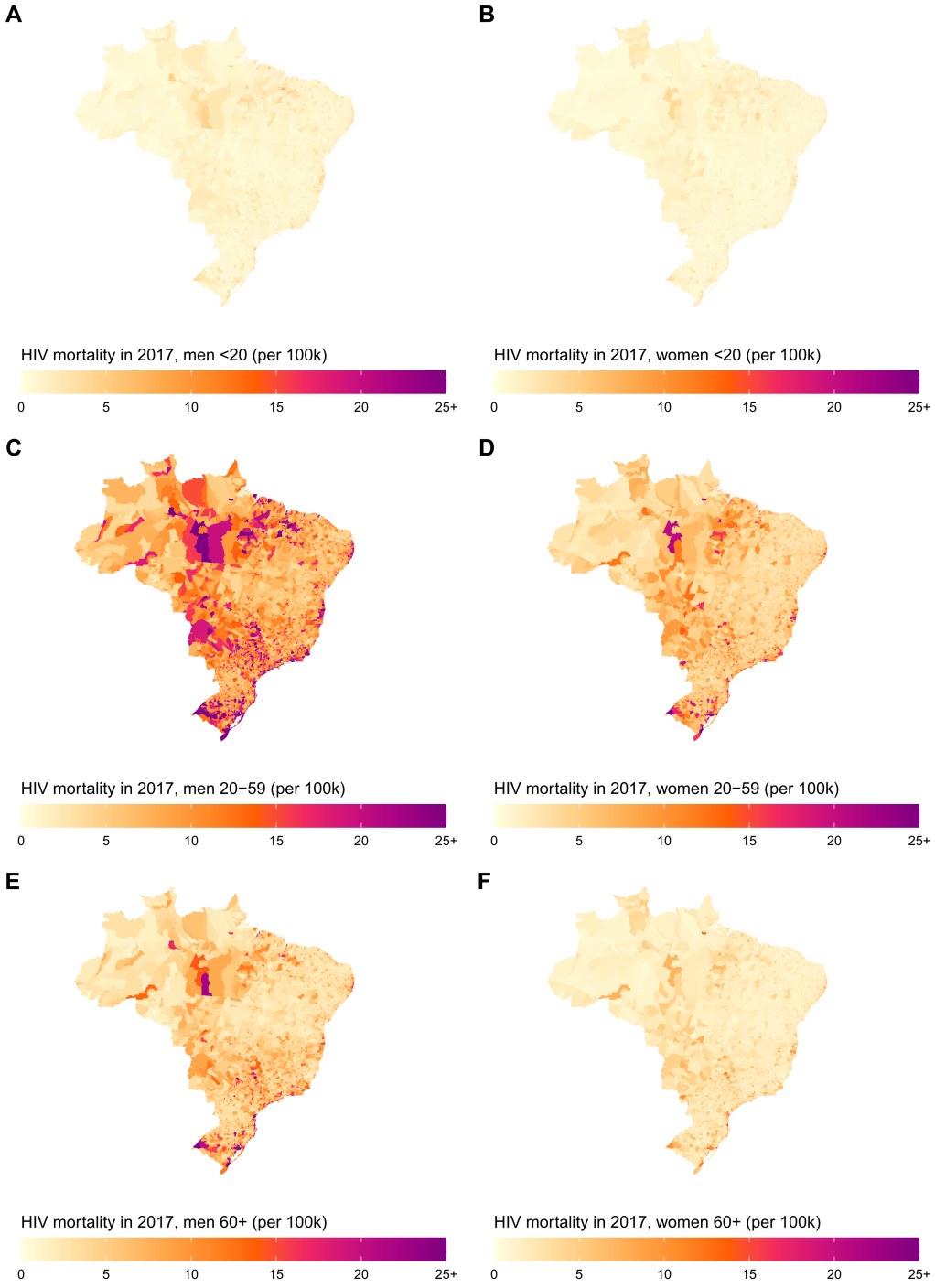

Figure S13: Estimated HIV mortality in Brazil by age group, 2017. Estimated HIV mortality at the municipality level in 2017 in Brazil among men (**a**) and women (**b**) less than 20 years of age, among men (**c**) and women (**d**) between 20 and 59 years of age, and among men (**e**) and women (**f**) over 60 years of age.

Figure S14: Estimated HIV mortality in Colombia by age group, 2017

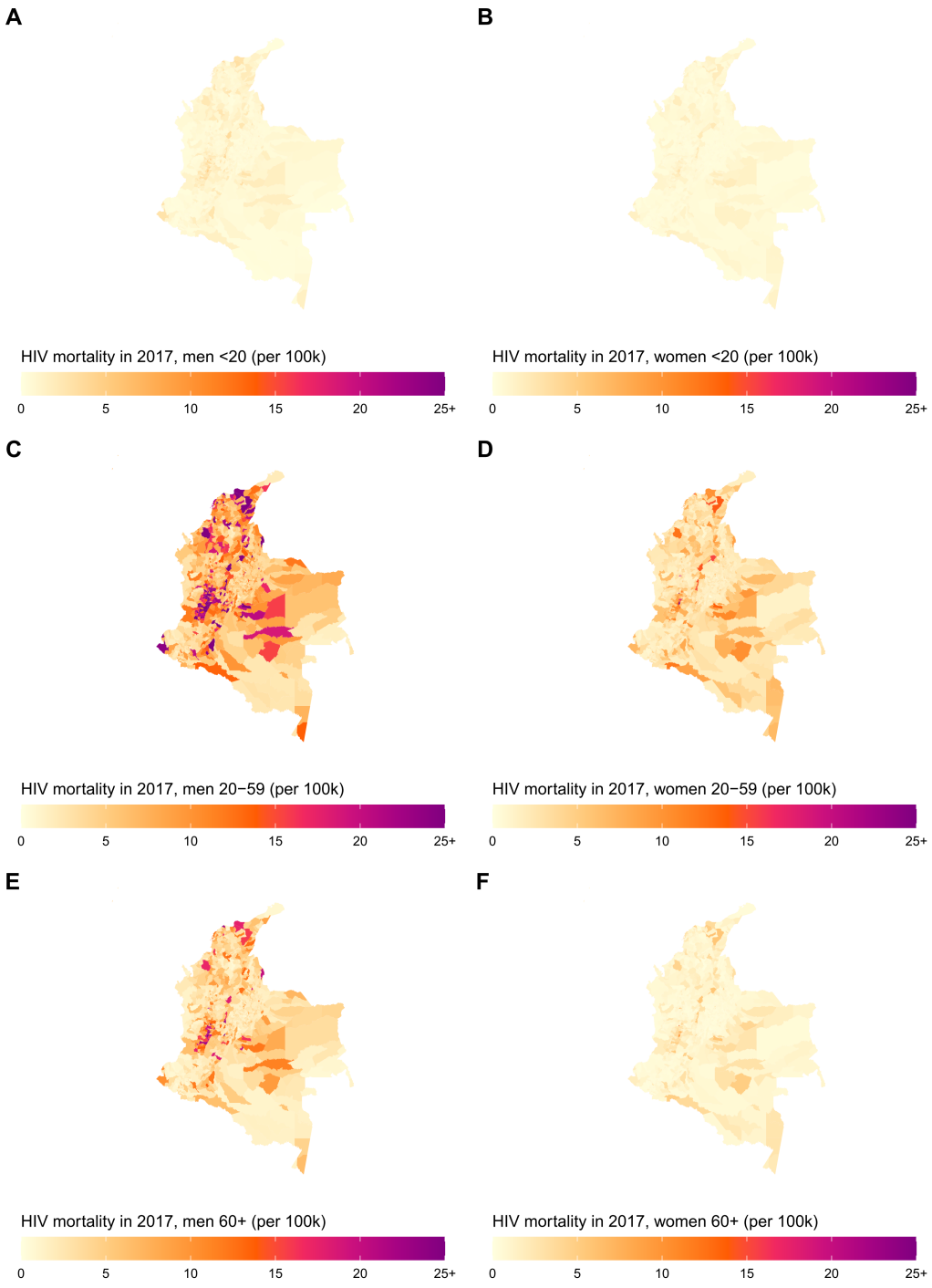

Figure S14: Estimated HIV mortality in Colombia by age group, 2017. Estimated HIV mortality at the municipality level in 2017 in Colombia among men (**a**) and women (**b**) less than 20 years of age, among men (**c**) and women (**d**) between 20 and 59 years of age, and among men (**e**) and women (**f**) over 60 years of age.

Figure S15: Estimated HIV mortality in Costa Rica by age group, 2016

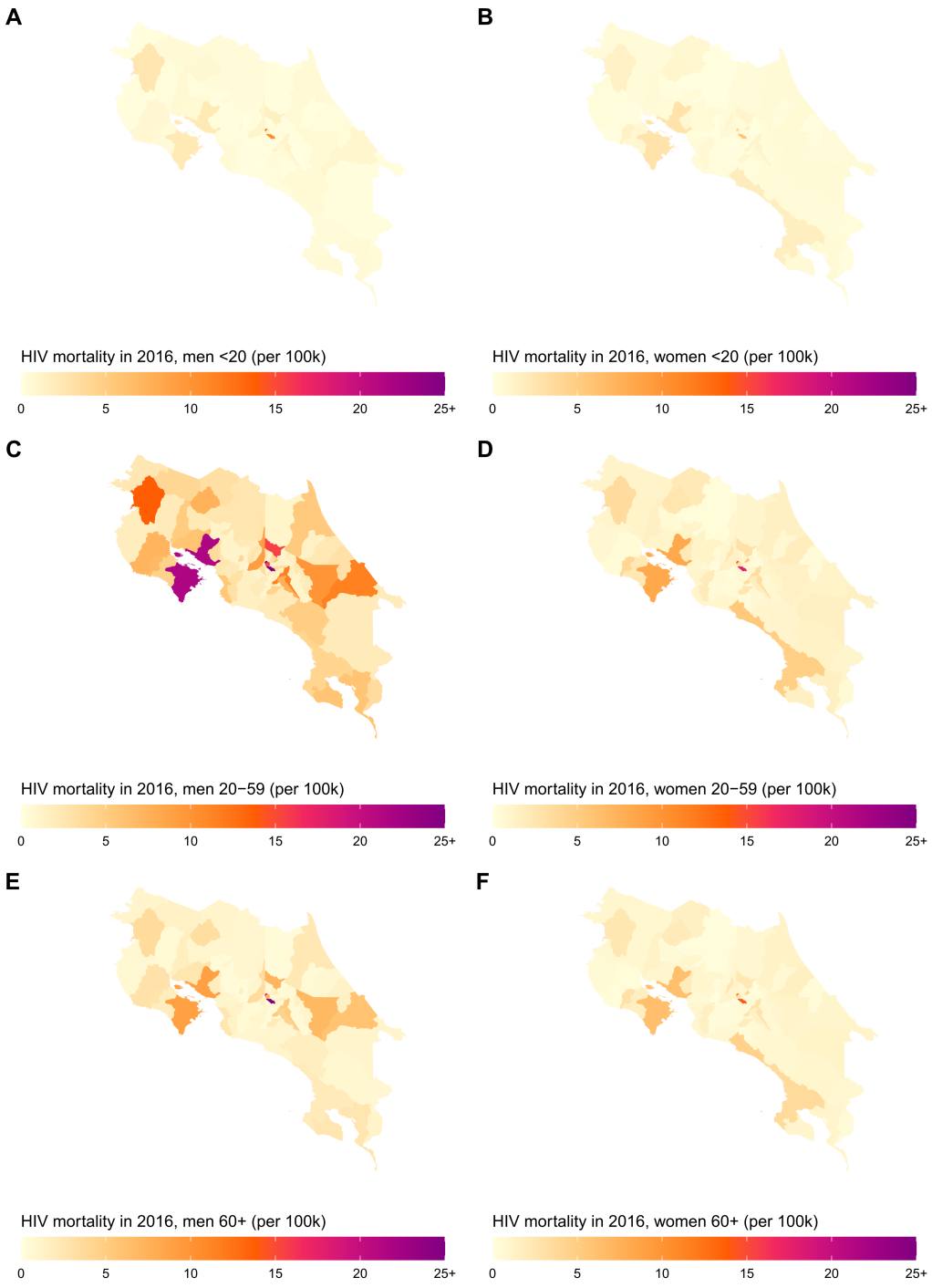

Figure S15: Estimated HIV mortality in Costa Rica by age group, 2016. Estimated HIV mortality at the canton level in 2016 in Costa Rica among men (**a**) and women (**b**) less than 20 years of age, among men (**c**) and women (**d**) between 20 and 59 years of age, and among men (**e**) and women (**f**) over 60 years of age.

Figure S16: Estimated HIV mortality in Ecuador by age group, 2014

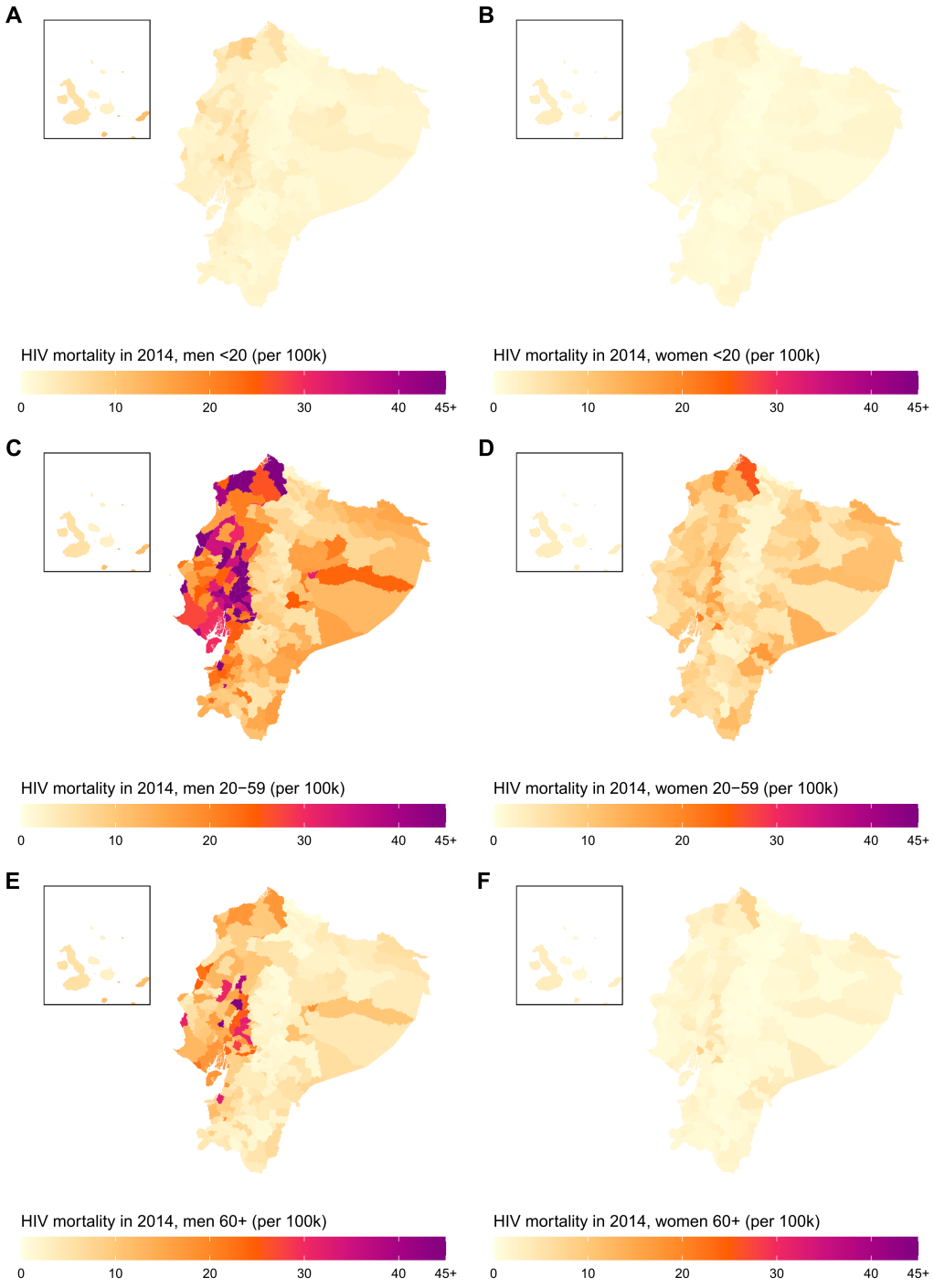

Figure S16: Estimated HIV mortality in Ecuador by age group, 2014. Estimated HIV mortality at the canton level in 2014 in Ecuador among men (**a**) and women (**b**) less than 20 years of age, among men (**c**) and women (**d**) between 20 and 59 years of age, and among men (**e**) and women (**f**) over 60 years of age.

Figure S17: Estimated HIV mortality in Guatemala by age group, 2017

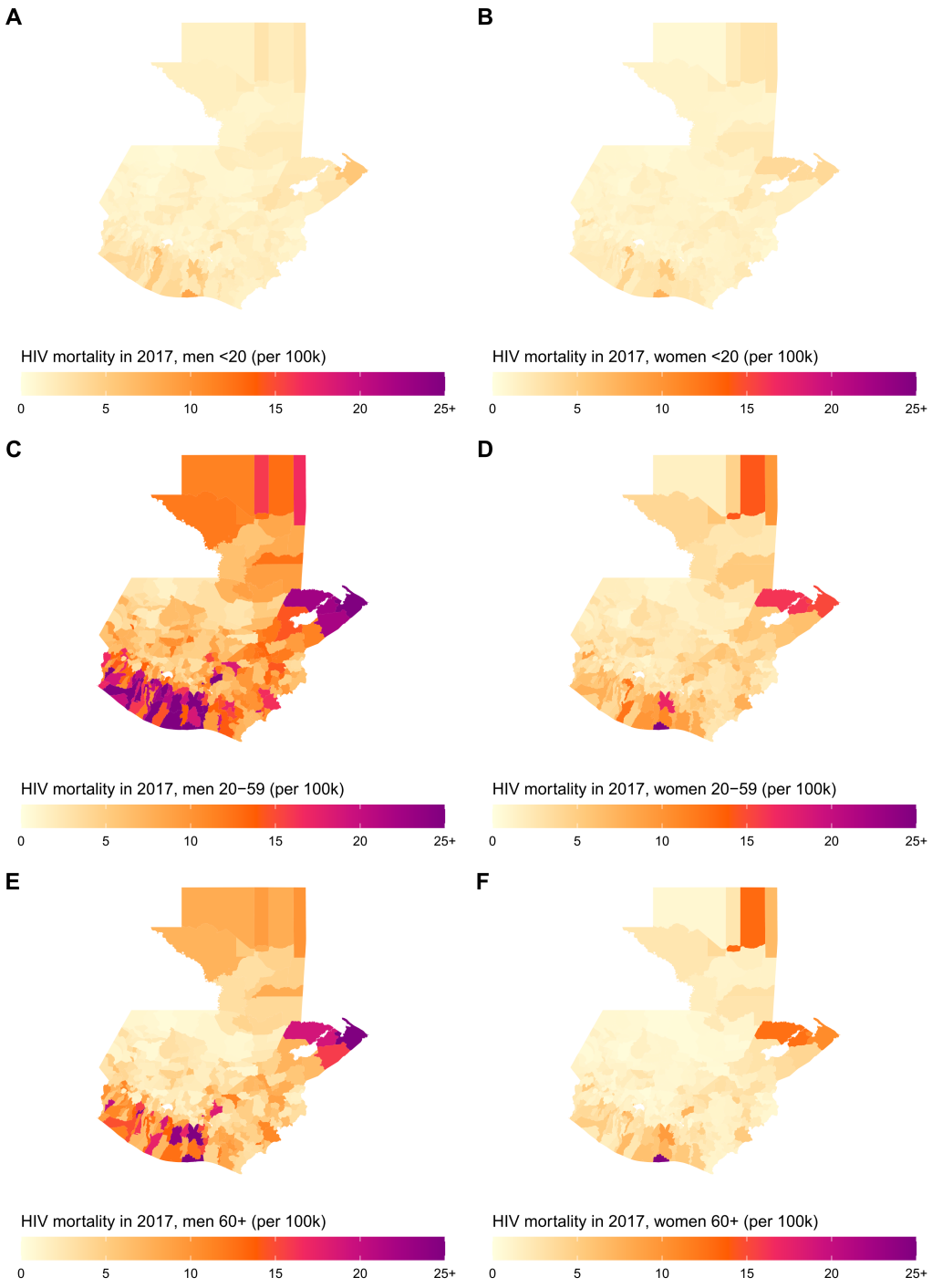

Figure S17: Estimated HIV mortality in Guatemala by age group, 2017. Estimated HIV mortality at the municipality level in 2017 in Guatemala among men (**a**) and women (**b**) less than 20 years of age, among men (**c**) and women (**d**) between 20 and 59 years of age, and among men (**e**) and women (**f**) over 60 years of age.

Figure S18: Estimated HIV mortality in Mexico by age group, 2017

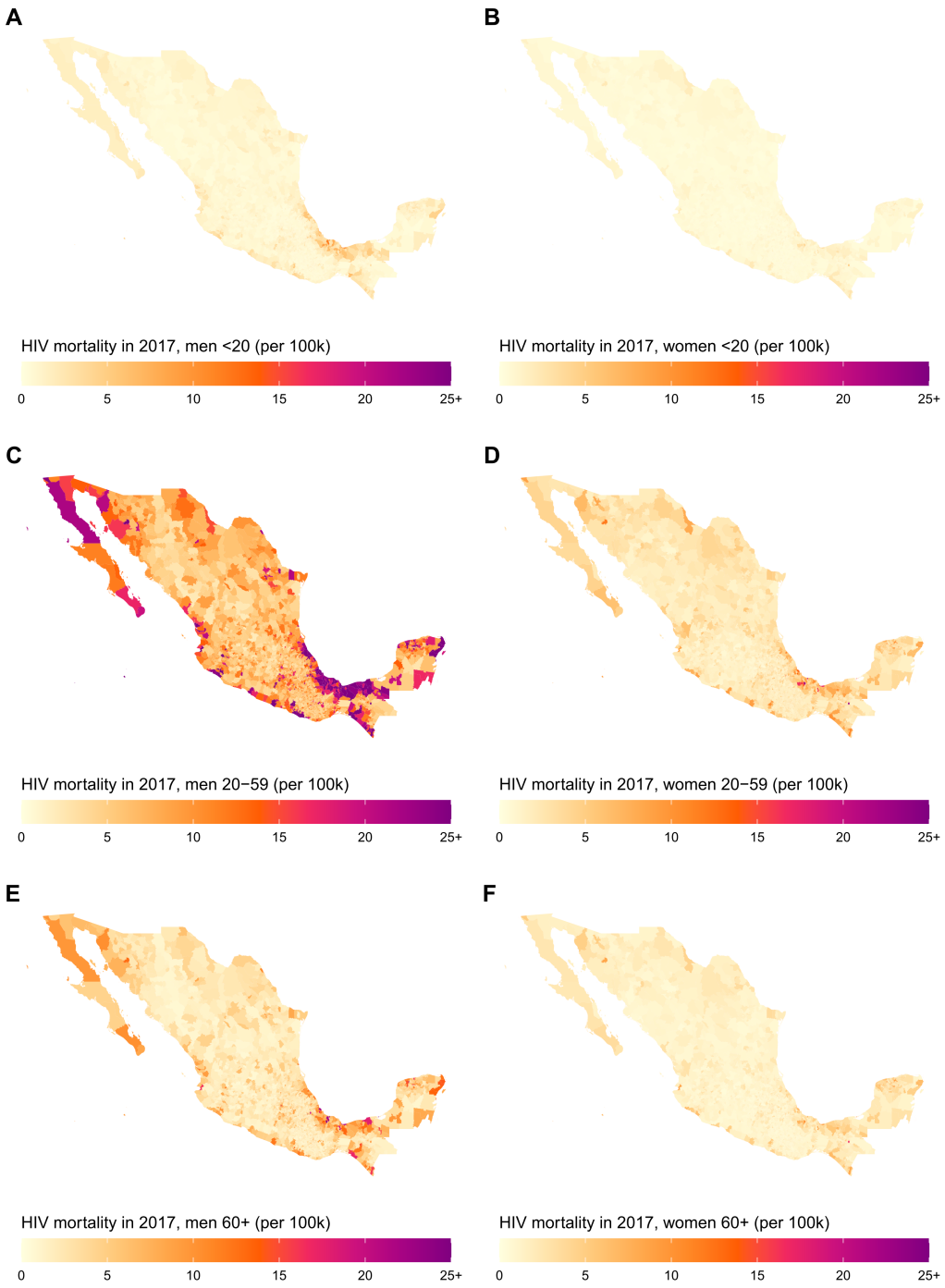

Figure S18: Estimated HIV mortality in Mexico by age group, 2017. Estimated HIV mortality at the municipality level in 2017 in Mexico among men (**a**) and women (**b**) less than 20 years of age, among men (**c**) and women (**d**) between 20 and 59 years of age, and among men (**e**) and women (**f**) over 60 years of age.

Supplementary tables

Table S1: Vital Registration data

Country	Year(s)	Reference	NID
Brazil	2000–2017	Ministry of Health (Brazil). Brazil Mortality Information System – Deaths 2000-2017. Rio de Janeiro, Brazil: Ministry of Health (Brazil).	153037,153038, 153039, 153040, 153041,153042, 153043,153044, 153045,153046, 153048,153049, 153050,173779, 265226, 268267, 317728, 386735
Costa Rica	2014–2016	National Institute of Statistics and Censuses (Costa Rica). Costa Rica Registered Deaths 2014-2016. San José, Costa Rica: National Institute of Statistics and Censuses (Costa Rica).	398942,325066, 398943
Colombia	2000–2017	National Administrative Department of Statistics (DANE) (Colombia). Colombia Vital Statistics - Deaths 2000-2017. Bogotá, Colombia: National Administrative Department of Statistics (DANE) (Colombia).	397407,397409, 397411, 397413, 397415, 397417, 397419, 397421, 65267, 65199, 57982, 265177, 265178, 265179, 265181, 265219, 265220, 396797
Ecuador	2004–2014	National Institute of Statistics and Censuses (Ecuador). Ecuador General Deaths 2004-2014. Quito, Ecuador: National Institute of Statistics and Censuses (Ecuador).	343283,343285, 343287,343289, 256676, 256677, 256678, 256679, 256680. 256681, 325080
Guatemala	2009–2017	National Statistics Institute (Guatemala). Guatemala Vital Statistics 2009-2017. Guatemala City, Guatemala: National Statistics Institute (Guatemala).	336252, 336251, 336250, 240728, 240729, 240730, 286175, 335901, 398900
Mexico	2000–2016	National Institute of Statistics and Geography (INEGI) (Mexico). Mexico Vital Registration - Deaths 2000-2016.	116138, 116139, 116140, 116141, 116142,116143, 116144, 116145, 116146, 93775, 116147, 107113, 124425, 157617, 240409, 281783, 325345, 386753

*NID = Data source unique identifier in the Global Health Data Exchange (http://ghdx.healthdata.org/). Additional information about each data sources is available via the GHDx, including information about the data provider and links to where the data can be accessed or requested (where available). NIDs can be entered in the search bar to retrieve the record for a particular source.

Table S2: Merged municipalities by country to form stable geographical units

Country	State	Group	Areas
Brazil	Para	1	Mojui dos Campos, Santarem
Brazil	Piaui	1	Altos, Pau D'Arco do Piaui
Brazil	Piaui	2	Aroeiras do Itaim, Picos
Brazil	Piaui	3	Nazaria, Teresina
Brazil	Rio Grande do Norte	1	Jundia, Varzea
Brazil	Alagoas	1	Coruripe, Jequia da Praia, Sao Miguel dos Campos
Brazil	Bahia	1	Barreiras, Luis Eduardo Magalhaes
Brazil	Bahia	2	Barrocas, Serrinha
Brazil	Espirito Santo	1	Colatina, Governador Lindenberg
Brazil	Rio de Janeiro	1	Mesquita, Nova Iguacu
Brazil	Santa Catarina	1	Criciuma, Balneario Rincao
Brazil	Santa Catarina	2	Laguna, Pescaria Brava
Brazil	Rio Grande do Sul	1	Acegua, Bage
Brazil	Rio Grande do Sul	2	Agua Santa, Caseiros, Ibiaca, Santa Cecilia do Sul, Tapejara
Brazil	Rio Grande do Sul	3	Almirante Tamandare do Sul, Carazinho
Brazil	Rio Grande do Sul	4	Arroio do Padre, Pelotas
Brazil	Rio Grande do Sul	5	Augusto Pestana, Boa Vista do Cadeado, Boa Vista do Incra, Bozano, Cruz Alta, Fortaleza dos Valos, Ijui
Brazil	Rio Grande do Sul	6	Barao de Cotegipe, Erechim, Jacutinga, Paulo Bento, Ponte Preta, Quatro Irmaos
Brazil	Rio Grande do Sul	7	Bento Goncalves, Pinto Bandeira, Pinto Bandeira
Brazil	Rio Grande do Sul	8	Caibate, Mato Queimado
Brazil	Rio Grande do Sul	9	Campinas do Sul, Cruzaltense
Brazil	Rio Grande do Sul	10	Canudos do Vale, Forquetinha, Lajeado, Progresso
Brazil	Rio Grande do Sul	11	Capao Bonito do Sul, Lagoa Vermelha
Brazil	Rio Grande do Sul	12	Capao do Cipo, Santiago, Sao Miguel das Missoes
Brazil	Rio Grande do Sul	13	Constantina, Novo Xingu
Brazil	Rio Grande do Sul	14	Coqueiro Baixo, Nova Brescia, Relvado
Brazil	Rio Grande do Sul	15	Coronel Pilar, Garibaldi, Roca Sales
Brazil	Rio Grande do Sul	16	Ernestina, Ibirapuita, Tio Hugo, Victor Graeff
Brazil	Rio Grande do Sul	17	Herval, Pedras Altas, Pinheiro Machado
Brazil	Rio Grande do Sul	18	Esmeralda, Pinhal da Serra
Brazil	Rio Grande do Sul	19	Espumoso, Jacuizinho, Salto do Jacui
Brazil	Rio Grande do Sul	20	Imigrante, Teutonia, Westfalia
Brazil	Rio Grande do Sul	21	Itati, Terra de Areia
Brazil	Rio Grande do Sul	22	Lagoa Bonita do Sul, Sobradinho
Brazil	Rio Grande do Sul	23	Marata, Montenegro, Salvador do Sul, Sao José do Sul
Brazil	Rio Grande do Sul	24	Palmeira das Missoes, Sao Pedro das Missoes
Brazil	Rio Grande do Sul	25	Rolador, Sao Luiz Gonzaga
Brazil	Rio Grande do Sul	26	Santa Margarida do Sul, Sao Gabriel

Brazil	Mato Grosso do Sul	1	Agua Clara, Camapua, Chapadao do Sul, Costa Rica, Figueirao, Paraiso das Aguas
Brazil	Mato Grosso	1	Agua Boa, Nova Nazare
Brazil	Mato Grosso	2	Alto Boa Vista, Bom Jesus do Araguaia, Cocalinho, Novo Santo Antonio, Ribeirao Cascalheira, Sao Felix do Araguaia, Serra Nova Dourada
Brazil	Mato Grosso	3	Aripuana, Colniza, Rondolandia
Brazil	Mato Grosso	4	Caceres, Curvelandia, Lambari D'Oeste, Mirassol d'Oeste
Brazil	Mato Grosso	5	Claudia, Itauba, Nova Santa Helena
Brazil	Mato Grosso	6	Conquista D'Oeste, Pontes e Lacerda, Vale de Sao Domingos
Brazil	Mato Grosso	7	Ipiranga do Norte, Itanhanga, Tapurah
Brazil	Mato Grosso	8	Nova Mutum, Santa Rita do Trivelato
Brazil	Mato Grosso	9	Novo Sao Joaquim, Santo Antonio do Leste
Brazil	Mato Grosso	10	Sao José do Xingu, Santa Cruz do Xingu
Brazil	Goias	1	Anapolis, Campo Limpo de Goias
Brazil	Goias	2	Ceres, Ipiranga de Goias
Brazil	Goias	3	Gameleira de Goias, Silvania
Brazil	Goias	4	Itaja, Lagoa Santa
Mexico	Guerrero	1	Azoyu, Cuajinicuilapa, Juchitan, Marquelia
Mexico	Guerrero	2	Chilapa de Alvarez, José Joaquin de Herrera
Mexico	Guerrero	3	Iliatenco, Malinaltepec, San Luis Acatlan
Mexico	Guerrero	4	Cochoapa el Grande, Metlatonoc
Mexico	Jalisco	1	Arandas, San Ignacio Cerro Gordo
Mexico	Mexico	1	Jaltenco, Tonanitla
Mexico	Mexico	2	San Felipe del Progreso, San José del Rincon
Mexico	Mexico	3	Luvianos, Tejupilco
Mexico	Quintana Roo	1	Bacalar, Othon P. Blanco
Mexico	Quintana Roo	2	Benito Juarez, Puerto Morelos
Mexico	Quintana Roo	3	Solidaridad, Tulum
Mexico	Veracruz de Ignacio de la Llave	1	Martinez de la Torre, San Rafael
Mexico	Veracruz de Ignacio de la Llave	2	Playa Vicente, Santiago Sochiapan
Mexico	Zacatecas	1	Santa Maria de la Paz, Teul de Gonzalez Ortega
Guatemala	Suchitepequez	1	Cuyotenango, San José La Maquina
Guatemala	San Marcos	1	La Blanca, Ocos
Guatemala	Huehuetenango	1	Concepcion Huista, Petatan
Guatemala	El Peten	1	La Libertad, Las Cruces
Guatemala	El Peten	2	Dolores, El Chal
Guatemala	Zacapa	1	San Jorge, Zacapa
Guatemala	Escuintla	1	La Gomera, Sipacate
Costa Rica	Puntarenas	1	Aguirre, Aguirre
Columbia	Bolivar	1	Norosi, Rio Viejo
Columbia	Cauca	1	Caloto, Guachene

Columbia	Cordoba	1	Montelibano, San José De Ure
Columbia	Cordoba	2	San Andres Sotavento, Tuchin
Columbia	Sucre	1	Covenas, Santiago De Tolu
Columbia	Amazonas	1	El Encanto, Puerto Alegria
Columbia	Guainia	1	Barranco Minas, Mapiripana
Ecuador	Los Rios	1	Quinsaloma, Ventanas
Ecuador	Pichincha, Santo Domingo De Los Tsachilas	1	Santo Domingo, Santo Domingo
Ecuador	Esmeraldas, Santo Domingo De Los Tsachilas, Zona No Delimitada	1	La Concordia, La Independencia, Plan Piloto, Quininde
Ecuador	Guayas, Santa Elena	1	Santa Elena, Santa Elena
Ecuador	Guayas, Santa Elena	2	La Libertad, La Libertad
Ecuador	Guayas, Santa Elena	3	Salinas, Salinas

Table S3: Covariate data sources

Covariate	Temporal resolution	Source	Reference	NID
Population Density	2000–2017	WorldPop	Geography and Environmental Science, University of Southampton, WorldPop. Age and Sex Structures, Global Per Country 2000-2020. Southampton, United Kingdom: WorldPop, 2018.	420764
Nighttime lights	2000–2013	NOAA DMSP	National Oceanic and Atmospheric Administration (NOAA) (United States), United States Air Force (USAF). DMSP-OLS Nighttime Lights Time Series, V4. United States of America: National Oceanic and Atmospheric Administration (NOAA) (United States).	418630
Travel time to the nearest settlement > 50,000 inhabitants	Null	Malaria Atlas Project, Big Data Institute, Nuffield Department of Medicine, University of Oxford	Nelson A, Joint Research Centre of the European Commission. Estimated travel time to the nearest city of 50,000 or more people in year 2000. Ispra, Italy: Global Environment Monitoring Unit, Joint Research Centre of the European Commission, 2008.	316680
Urbanicity	2000–2015	European Commission/ GHS	Pesaresi, Martino; Freire, Sergio (2016): GHS settlement grid, following the REGIO model 2014 in application to GHSL Landsat and CIESIN GPW v4-multitemporal (1975-1990-2000-2015). European Commission, Joint Research Centre (JRC) [Dataset] PID: http://data.europa.eu/89h/jrc-ghsl-ghs_smod_pop_globe_r2016a	418851

*NID = Data source unique identifier in the Global Health Data Exchange (http://ghdx.healthdata.org/). Additional information about each data sources is available via the GHDx, including information about the data provider and links to where the data can be accessed or requested (where available). NIDs can be entered in the search bar to retrieve the record for a particular source.